

AD-A024 378



AD

EDGEWOOD ARSENAL CONTRACTOR REPORT  
EM-CR-76043  
Report No. 9

DESIGN STUDY OF A SUPPRESSIVE STRUCTURE  
FOR A MELT LOADING OPERATION

by  
W. E. Baker  
P. A. Cox  
E. D. Esparaza  
P. S. Westine

TECHNICAL  
LIBRARY

December 1975

19970929 159

SOUTHWEST RESEARCH INSTITUTE  
Post Office Drawer 28510, 8500 Culebra Road  
San Antonio, Texas 78284

Contract No. DAAA15-75-C-0083

DEPARTMENT OF THE ARMY  
Headquarters, Edgewood Arsenal  
Aberdeen Proving Ground, Maryland 21010



Approved for public release; distribution unlimited

BEST AVAILABLE COPY

DTIC QUALITY INSPECTED 1

Incl 3

Disclaimer

The findings in this report are not to be construed as an official Department of the Army position unless so designated by other authorized documents.

Disposition

Destroy this report when it is no longer needed. Do not return it to the originator.

UNCLASSIFIED

SECURITY CLASSIFICATION OF THIS PAGE (When Data Entered)

REPORT DOCUMENTATION PAGE		READ INSTRUCTIONS BEFORE COMPLETING FORM
1. REPORT NUMBER EM-CR-76043	2. GOVT ACCESSION NO.	3. RECIPIENT'S CATALOG NUMBER
4. TITLE (and Subtitle)  DESIGN STUDY OF A SUPPRESSIVE STRUCTURE FOR A MELT LOADING OPERATION		5. TYPE OF REPORT & PERIOD COVERED Technical Report
		6. PERFORMING ORG. REPORT NUMBER Report No. 9
7. AUTHOR(s) W.E. Baker, P.A. Cox E.D. Esparza and P.S. Westine		8. CONTRACT OR GRANT NUMBER(s)  DAAA15-75-C-0083
9. PERFORMING ORGANIZATION NAME AND ADDRESSES Southwest Research Institute P. O. Drawer 28510 San Antonio, Texas 78284		10. PROGRAM ELEMENT, PROJECT, TASK AREA & WORK UNIT NUMBERS  PA, A 5751265
11. CONTROLLING OFFICE NAME AND ADDRESS Commander, Edgewood Arsenal Attn: SAREA-TS-R Aberdeen Proving Ground, Maryland 21010		12. REPORT DATE December 1975
		13. NUMBER OF PAGES 74
14. MONITORING AGENCY NAME & ADDRESS (if different from Controlling Office) Commander, Edgewood Arsenal Attn: SAREA-MT-H Aberdeen Proving Ground, MD 21010 (CPO Mr. Bruce W. Jezek 671-2661)		15. SECURITY CLASS. (of this report)  UNCLASSIFIED
		15a. DECLASSIFICATION/DOWNGRADING SCHEDULE  NA
16. DISTRIBUTION STATEMENT (of this Report)  Approved for public release; distribution unlimited		
17. DISTRIBUTION STATEMENT (of the abstract entered in Block 20, if different from Report)		
18. SUPPLEMENTARY NOTES		
19. KEY WORDS (Continue on reverse side if necessary and identify by block number)  Suppressive structures                      Fragment attenuation Category 1 structures                      Blast Loading Plastic design                              Quasi-static loading Blast attenuation		
20. ABSTRACT (Continue on reverse side if necessary and identify by block number)  This report presents the results of a design study for a structure to suppress blast and fragment effects from detonation of a large quantity of Comp B explosive in a melt kettle. A number of design concepts were evaluated, and a specific configuration recommended. Relatively detailed design drawings were prepared.		

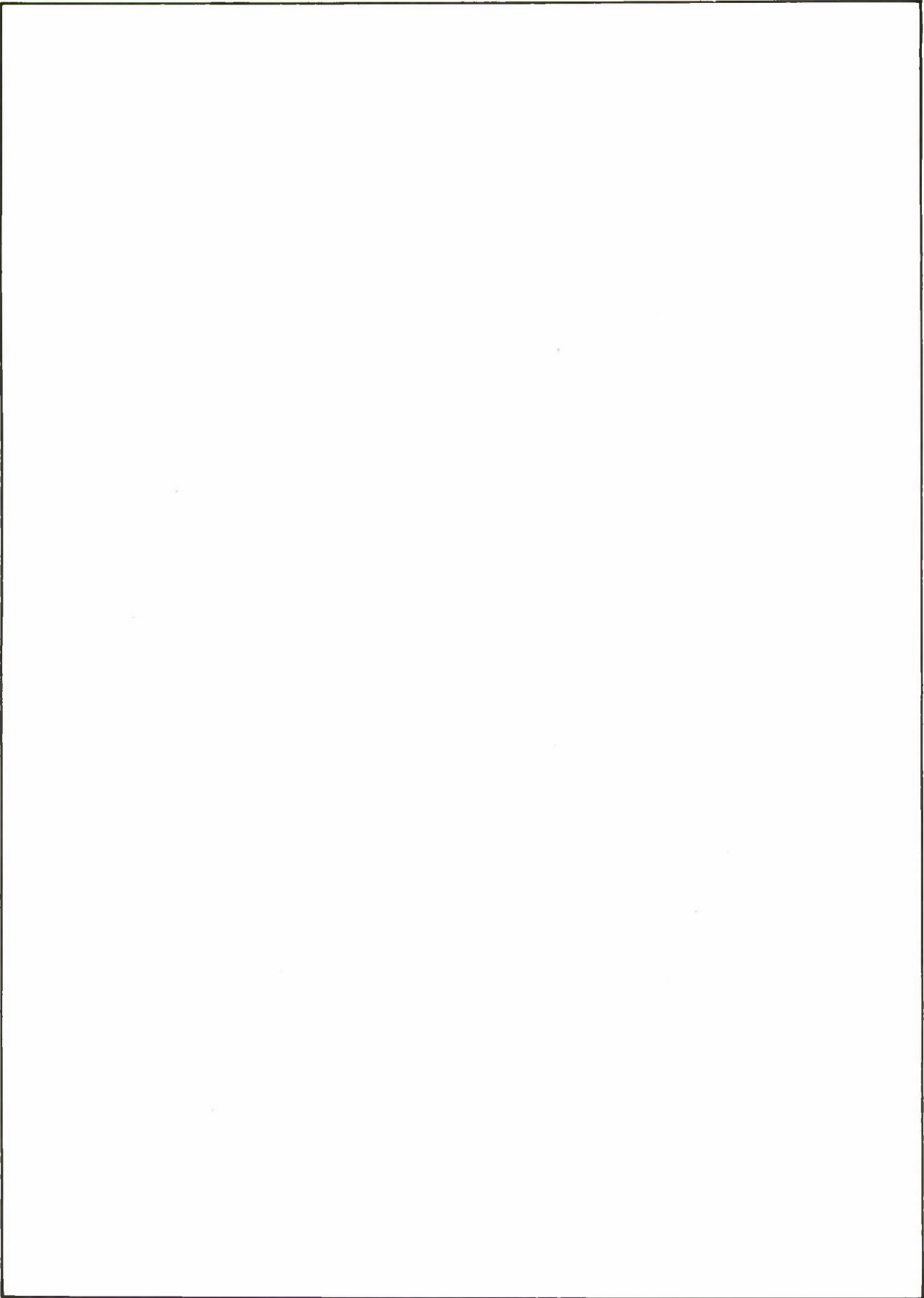
DD FORM 1473  
1 JAN 73

EDITION OF 1 NOV 65 IS OBSOLETE

UNCLASSIFIED

SECURITY CLASSIFICATION OF THIS PAGE (When Data Entered)

SECURITY CLASSIFICATION OF THIS PAGE (When Data Entered)



SECURITY CLASSIFICATION OF THIS PAGE (When Data Entered)

## SUMMARY

This report documents the results of a study to design a structure which suppresses the blast effects and defeats the fragments from the detonation of 3125 lb of Composition B explosive in a melt kettle. Blast suppression is to 50% or better of the peak free-field side-on overpressure at the intraline distance (from DOD standard). The fragment which the structure must defeat is a 1-lb mass traveling at 7200 fps (Reference 1). Called a suppressive shield, the structure will house a melt pour operation which requires about 1600 sq. ft. of floor area and a volume of about 64,000 ft<sup>3</sup>.

Two basic design concepts with equal internal volume and floor area were considered. The first was a cubical structure 40 ft. on a side with maximum venting from the four walls and the roof. The second concept was a cylindrical design, approximately 40 ft. in height, and 45 ft. in diameter. From this basic cylindrical configuration, different vented sidewalls and different vented and unvented roofs were studied in an attempt to optimize the design. The alternative designs considered and a brief description of each are:

### Cylindrical sides (with venting):

**Vertical I-beams**—Interlocking I-beams are banded together by circumferential rings which react the internal pressure loads. I-beam flanges defeat the fragments and spacing controls the venting.

**Perforated plate**—Concentric perforated cylinders react the internal pressure loads. Angles are stacked inside the cylinders to aid in defeating the fragments.

### Roof designs:

**Membrane (with venting)**—Three spaced layers of perforated plate defeat the fragments and react the blast loading in membrane action.

**Lifting or pop-up (with venting)**—The roof is allowed to rise from the vertical cylinder to reduce the strength requirements of the roof and eliminate problems of attachment to the cylinder.

**Interlocking I-beams (with venting)**—Designed to resist the blast loading in bending, this concept utilizes large beams arranged radially like spokes in a wheel with interlocking I-beams arranged circumferentially between the spokes. The interlocking I-beams in this concept are the same as those used in the vertical I-beam cylinder.

**Double-dome (non-venting)**—Two concentric domes, with a filler material in between, form the roof on the cylinder in this concept. Fragments are defeated by the inner dome and filler material and the blast loads are reacted by the outer dome.

A flat reinforced concrete slab, designed by the Corps of Engineers, Huntsville, Alabama, is used as the foundation for the cylindrical design. In the design for the cubical shield, the floor is constructed of steel in the same manner as the walls and roof so that no additional foundation is required.

Although both the box configuration and the cylindrical configuration are structurally feasible for the Category 1 shield, a much lighter structure in terms of steel weight is achieved by the cylindrical design. Of the alternative designs considered for the cylindrical configuration, the cylinder of interlocking I-beams and the dome roof produced the most economical structure. Cost comparisons were based primarily on steel weight but also upon discussions with steel fabricators who reviewed the conceptual drawings. On the basis of steel weight, the box configuration and the recommended cylindrical configuration compare as follows:

Box configuration:	1721 tons
Cylindrical configuration:	495 tons

Foundation reinforcing steel is not included in the weight for the cylindrical design.

We believe that the cylindrical configuration with the dome roof is near optimum for a partially vented structure which suppresses the blast effects of 3125 lb of Composition B explosive and defeats the primary fragment. However, more efficient structures can perhaps be achieved in a full containment\* rather than partially vented shield. For full containment the sand-filled double-wall design, found to be efficient for the dome roof, could be utilized for the cylindrical section of the shield also.

A development program is recommended for dome-type roofs in vented cylindrical configurations as well as for fully closed cylindrical and/or spherical shields utilizing the double wall construction. In addition, footing type foundations as an alternative to slab type foundations should be investigated. Footing type foundations would permit more flexibility in the use of internal space because large pits could be recessed in the floor to accommodate equipment which would otherwise have to be placed above grade.

## PREFACE

The investigation described in this report was authorized under PA, A 4932, Project 5751264. The work was performed at Southwest Research Institute under Contract DAAA15-75-C-0083.

The use of trade names in this report does not constitute an official endorsement or approval of the use of such commercial hardware or software. This report may not be cited for the purposes of advertisement.

The information in this document has been cleared for release to the general public.

\*Some small amount of venting may still occur through access doors and other openings.

## TABLE OF CONTENTS

	Page
LIST OF ILLUSTRATIONS . . . . .	6
LIST OF TABLES . . . . .	7
I. INTRODUCTION . . . . .	9
II. DESIGN REQUIREMENTS . . . . .	10
III. DESIGN CONCEPTS . . . . .	11
A. Review of Previous Design Analysis on Contract No. DAAD05-74-C-0751 . . . . .	11
B. Design Alternatives Considered on Present Contract . . . . .	12
1. <i>Rectangular Box Concepts</i> . . . . .	12
2. <i>Vertical Cylinder Concepts</i> . . . . .	19
C. Alternate Cylinder and Roof Configurations . . . . .	23
1. <i>I-Beam Cylinder</i> . . . . .	24
2. <i>Perforated Cylinder</i> . . . . .	25
3. <i>Membrane Roof</i> . . . . .	31
4. <i>Lifting Top</i> . . . . .	31
5. <i>I-Beam Roof</i> . . . . .	33
6. <i>Double-Dome Roof</i> . . . . .	37
IV. RESULTS . . . . .	41
A. General Discussion . . . . .	41
B. Design Comparisons . . . . .	41
V. CONCLUSIONS AND RECOMMENDATIONS . . . . .	45
APPENDICES	
A. Methods of Estimating Dynamic and Static Loading . . . . .	47
B. Methods of Estimating Structural Response . . . . .	51
C. Methods for Estimating Fragment Penetration . . . . .	67
D. Errata in Chapter 6 . . . . .	71
REFERENCES . . . . .	73

## LIST OF ILLUSTRATIONS

Figure		Page
1	Quarter-Scale Frame for Rectangular Box Structure . . . . .	14
2	Modified Quarter-Scale Frame for Rectangular Box Structure . . . . .	15
3	Cross-Section of Frame Vertical Members in Quarter-Scale Box Structure . . . . .	16
4	Cross Section of I-Beam Panel <sup>2</sup> . . . . .	18
5	Typical Panel Installation in Box Structure . . . . .	20
6	Cylindrical Concept . . . . .	21
7	Door and Assembly Details of the I-Beam Cylinder . . . . .	26
8	Perforated Cylinder . . . . .	29
9	Door Details for Perforated Cylinder . . . . .	30
10	Attachment of Membrane Roof to I-Beam Cylinder . . . . .	32
11	Height of Rise of Restrained Roof . . . . .	34
12	Quasi-Static Pressure for Lifting Roof Design . . . . .	35
13	I-Beam Roof Concept . . . . .	36
14	Double-Dome Roof Concept . . . . .	38
15	Final Cylindrical Concept Suggested for Category I Prototype . . . . .	39
16	Sand Filled Double-Dome Roof . . . . .	42
A-1	Curve Fit to Blast Pressures Outside NSTL Structures . . . . .	50
B-1	Schematic of Error Incurred in Assuming Simultaneity of Loading and Constant Quasi-Static Pressure . . . . .	55
B-2	Schematic of Cases Analyzed for Coupled Beam-Ring Response . . . . .	57
B-3	Radial Deflection of Center Ring-Category I Cylindrical Shield with W8 X 67 Beams . . . . .	59

## LIST OF ILLUSTRATIONS (Cont'd)

Figure		Page
B-4	Lumped-Parameter Model of Segment from the I-Beam Roof Concept . . .	61
B-5	Model of the Membrane Roof . . . . .	62
B-6	Vertical Deflections of the Membrane Roof Concept . . . . .	63
B-7	Member Axial Strains in the Membrane Roof Concept . . . . .	64
C-1	Fragment Containment for $W/W_c = 1$ . . . . .	70

## LIST OF TABLES

Table		Page
I	Summary of SwRI Panel Concepts . . . . .	17
II	Breakdown of Steel Weight (in Tons) for Prototype Category 1 Concepts . . .	43
III	Weight Comparison of Cube Concept with Final Cylindrical Concept for Category I Prototype Suppressive Shield . . . . .	44
A-1	Loading on Full-Scale Category 1 Suppressive Structure . . . . .	49
B-1	Summary of Energy Solutions for Estimating Plastic Deformation of Blast-Loaded Elements . . . . .	52
B-2	Definition of Symbols used in Table B-1 . . . . .	54
B-3	Summary of Computer Calculations for Coupled Beam-Ring Response . . .	58

# DESIGN STUDY OF A SUPPRESSIVE STRUCTURE FOR A MELT LOADING OPERATION

## I. INTRODUCTION

This report presents the results of a design study for a structure which suppresses the blast effects and defeats the fragments produced by an accidental detonation of a relatively large quantity of explosive. The work is a follow-on to the studies documented in Technical Report No. 1 on Contract DAAD05-74-C-0751 which included analyses and preliminary designs of a suppressive structure for a melt loading operation.<sup>(1)\*</sup> The current work was done on Contract DAAA15-75-C-0083 for the Edgewood Arsenal Suppressive Structure Program.

To facilitate the application of suppressive structures to Army ammunition plants, Edgewood Arsenal has established a generic set of suppressive structures termed "category shields". The structure for application to melt pour operation is the Category 1 shield. The blast and fragment hazards are defined for each category shield with the Category 1 shield hazards described as severe fragments, and peak side-on blast pressures at the wall between 500 and 1200 psi. The particular application of the Category 1 shield covered in this report is a melt pour operation which processes 2500 lb of Composition B explosive. With a 25% overcharge requirement the design charge weight is 3125 lb resulting in a peak side-on overpressure of 550 psi. Specific design requirements are given in Section II.

Two basic design concepts were considered for the shield. The first was a cubical structure 40 ft on a side with maximum venting from the four walls and the roof. The second basic concept was a cylindrical design 40 ft in height with the same working floor area as the cubical structure. This resulted in a 45-foot diameter cylinder. From the basic cylindrical configuration, different vented sidewalls and different vented and unvented roofs were studied in an attempt to optimize the design.

Early in the study, venting requirements for the shield were established by the empirical method developed in Reference 1. In later phases of the program, results from tests conducted by BRL, for structures which were 1/16-scale of the full-scale rectangular concept, were reduced to nondimensional form and used to establish the venting requirements for the shield designs.

Loads on the shield include those associated with the initial blast wave plus those produced by the longer duration quasi-static pressure rise. The peak quasi-static pressure and venting time for the structure were obtained from Reference 1. Additional data from the literature were also utilized to develop an alternate method for predicting venting times. This new method covers a wider range of venting parameters than the method of Reference 1. Initial blast loads on the inner surface of the shield were predicted from sources of reflected blast data in the open literature.

\*Numbers indicate references listed at the end of this report.

Many of the design formulas documented in Reference 1 were updated and improved during the current study. Revisions were based either on new and better data or upon the inclusion of phenomena that may have been omitted in the earlier study. In addition, new design formulas were developed as required to account for structural elements analyzed in this study that were not considered in the earlier work. These included formulas for rings supporting the I-beams in the cylindrical structure, as well as single hemispheres or double hemispheres separated by a filler material. Also, response calculations were made using existing computer programs developed at SwRI to study cases of coupled response not covered by the formulas or to generate results for comparison with the formulas.

This report has covered a time of evolution and development of the suppressive shield. Thus, the design philosophy was changing during this period, and these changes had a significant impact on the design of the Category 1 structure. Three distinct design approaches were followed. In chronological order, these were:

- The design of a fully vented shield of rectangular or box configuration,
- The design of a fully vented shield of cylindrical configuration,
- The design of a partially vented shield of cylindrical configuration.

Full venting included maximum venting of all interior surfaces of the shield except the floor, consistent with proper reduction of external overpressures. Partially vented structures included non-venting roofs as well as floors. The effects of these design changes will be obvious throughout the report.

In addition to the design requirements for the suppressive structure covered in Section II, this report includes some details of various design concepts which we considered (Section III), the results of the study (Section IV), and our conclusions and recommendations (Section V). Details of methods of estimating dynamic and static loading, penetration of fragments, and structural response are given in Appendices, plus other ancillary information.

## II. DESIGN REQUIREMENTS

The basic problem was described in Reference 1 together with a preliminary analysis and design of a Category 1 suppressive structure for a specific application in a melt loading plant. The general requirements for a Category 1 suppressive structure are that it must remain intact under the effects of an internal explosion which subjects it to side-on overpressures in the range of 500-1200 psi and to a severe fragment hazard.

The guidelines used for this study were:

- (1) Suppress the blast from 3,125 lb of Composition B explosive detonated in a melt kettle to 50% or better of the peak side-on overpressure at the intraline distance (from DOD standards) and at all closer distances.

- (2) Defeat the primary fragment defined as a 1-lb mass traveling at 7200 ft per second.
- (3) Build the shield to accommodate a floor working area of approximately 1,600 sq ft with an internal volume of about 64,000 cu ft.
- (4) Utilize the results of past studies, but include new concepts as appropriate. Configurations included box and cylindrical type structures, either fully or partially vented.
- (5) Design for gross plastic deformations short of failure in order to minimize structural weight.

Although there was some variation in loads depending on the particular configuration, the basic internal loads for which the prototype shield was designed are

Quasi-static pressure:	165 psi
Peak reflected pressure:	4,053 psi
Peak reflected impulse:	2.43 psi-sec

As in Reference 1, we used the current and past work on suppressive structures to predict the loading on the structure and to predict plastic structural deformations using limit design methods. Various configurations were assessed, and a final configuration recommended. Relatively detailed design drawings were made for both the full-scale structure and a one-quarter scale dynamic model. Factors considered in choosing a final design, in addition to the guidelines, were relative costs of different concepts and ease or difficulty of fabrication.

### III. DESIGN CONCEPTS

#### A. Review of Previous Design Analysis on Contract No. DAAD05-74-C-0751

The basic design concepts considered previously were:

- a. Rectangular box structure
- b. Horizontal cylindrical structure

These concepts employed deep-section steel framework members supporting suppressive (vented) panels of various designs. Members were sized to withstand impulsive and quasi-static internal pressures, but allowed to undergo considerable plastic deformation based on limit design formulas for structural members which were developed under the earlier contract. The response of vented panels in the structure was predicted using these limit design formulas; however, these panels were sized to contain the "worst case" fragment and were overdesigned

for the internal pressure loading. Few details of structural or foundation design were developed, and no estimates were made of relative costs of various concepts.

Concurrently with this previous SwRI study, Coutinho, et al.<sup>(2)</sup> also developed a rectangular box structural concept for the same Category 1 application. They considered fragment hazards as well as blast, but used a somewhat different philosophy of preliminary structural design. The deep frame members were designed to remain elastic. A new concept for vented panel design was advanced in Reference 2, that of interlocking I-beams.

SwRI supported the AMSAA design effort particularly their work on the Category 1 1/4-scale test structure. A brief description of this work follows:

- Review of AMSAA truss concept from Reference 2. This review included analysis of some truss components and bolted joints.
- Review and analysis of the AMSAA “heavy frame” I-beam concept. Results are documented in a letter by Baker.<sup>(3)</sup>
- Design study of a foundation for the 1/4-scale structure which had multiple-shot capability.
- Investigation of load attenuation on the frame of the 1/4-scale structure to be achieved by spring mounting the AMSAA I-beam panels.

## B. Design Alternatives Considered on Present Contract

We evaluated and designed a number of suppressive shield concepts, retaining the basic rectangular and cylindrical geometries from the earlier contract and considering both conventional and I-beam configurations for the vented panels. The cylindrical configurations changed from horizontal to vertical cylinders. Both blast and fragment loading were considered for all concepts. Design studies were usually conducted in either full scale or one-quarter scale with either structure being a simple geometric ratio of the other; however, in some cases where the prototype and one-quarter scale structures do not scale exactly, as is the case for the beams in the cylindrical concept, analysis of the prototype and one-quarter scale structures proceeded concurrently. The various concepts will now be discussed in some detail.

### 1. *Rectangular Box Concepts*

A number of iterations were made to design the preliminary rectangular concepts of References 1 and 2. Basic blast loads considered were\*:

$$\text{Initial reflected impulse } I_r = 2.43 \text{ psi-sec.}$$

\*See Appendix A for details of load development.

Initial reflected pressure  $P_r = 4053$  psi

Quasi-static pressure  $P_{Q_s} = 165$  psi

and the fragment hazard to be defeated was:

1-lb fragment impacting at an arbitrary obliquity at 7200 ft/sec

Basic design formulas from Reference 1 and later analyses\* at SwRI were used to size members to resist blast loads, while formulas from Reference 4 were used to determine panel configurations which would arrest the assumed worst case fragment.† The various frame and panel designs evolved into two frames and four panels. These designs are discussed in some detail in a paper by Cox and Esparza,<sup>(5)</sup> which will be paraphrased here.

The basic design procedure was to design full-scale, all steel structures to the loads noted above, and then to produce a quarter-scale replica‡ of this structure, using standard structural members as much as possible. Deep section I-beam or truss members were discarded early in the frame design to obviate problems of dynamic buckling, and relatively compact box sections were chosen instead. Also, to simplify foundation design, the frame members were carried completely around the structure so that the foundation need only be designed to carry the dead weight of the structure. Figures 1 and 2 show the final frame concepts, dimensioned for the quarter-scale model. The frame shown in Figure 1 has intersecting frame members in roof and floor, while the modified frame in Figure 2 has nested members to reduce welding fabrication. Because no standard structural members of compact section could be found to withstand the loads in some parts of the frames, doubler plates were welded to the standard box members as shown in Figure 3. In full-scale (four times the dimensions of the values in Figure 3) these members must be fabricated from plate because no standard box beams of this size are made commercially.

The four panel concepts were all designed to arrest the worst-case fragment and to withstand separately impulsive and quasi-static blast loads. No synergistic effects were considered, i.e., no combined fragment and blast effects, nor response to a complete pressure-time history. The designs are summarized in Table I with the elements that make up the panels given for both the full-scale panels and the quarter-scale model. For completeness, we also show in Figure 4 the schematic cross-section of an I-beam panel from Reference 2, even though we did not design it. The panels were originally designed to criteria which resulted in an effective vent area ratio,  $\alpha_e$ , giving a predicted blast wave suppression to 5 psi side-on overpressure at 75 ft from the structure. Later revisions in the panel designs increased the venting areas to achieve 50% or more blast pressure reduction at the intraline distance of 244 ft.

Attachment of the panels to the frame of Figure 2 varies with the panel design. For example, panels constructed with I-beams can be placed against the inside surface of the

\*See Appendix B for details of response analyses.

†See Appendix C for fragment penetration calculations

‡A "replica" is an exact geometrical model which is also made of all the same materials.

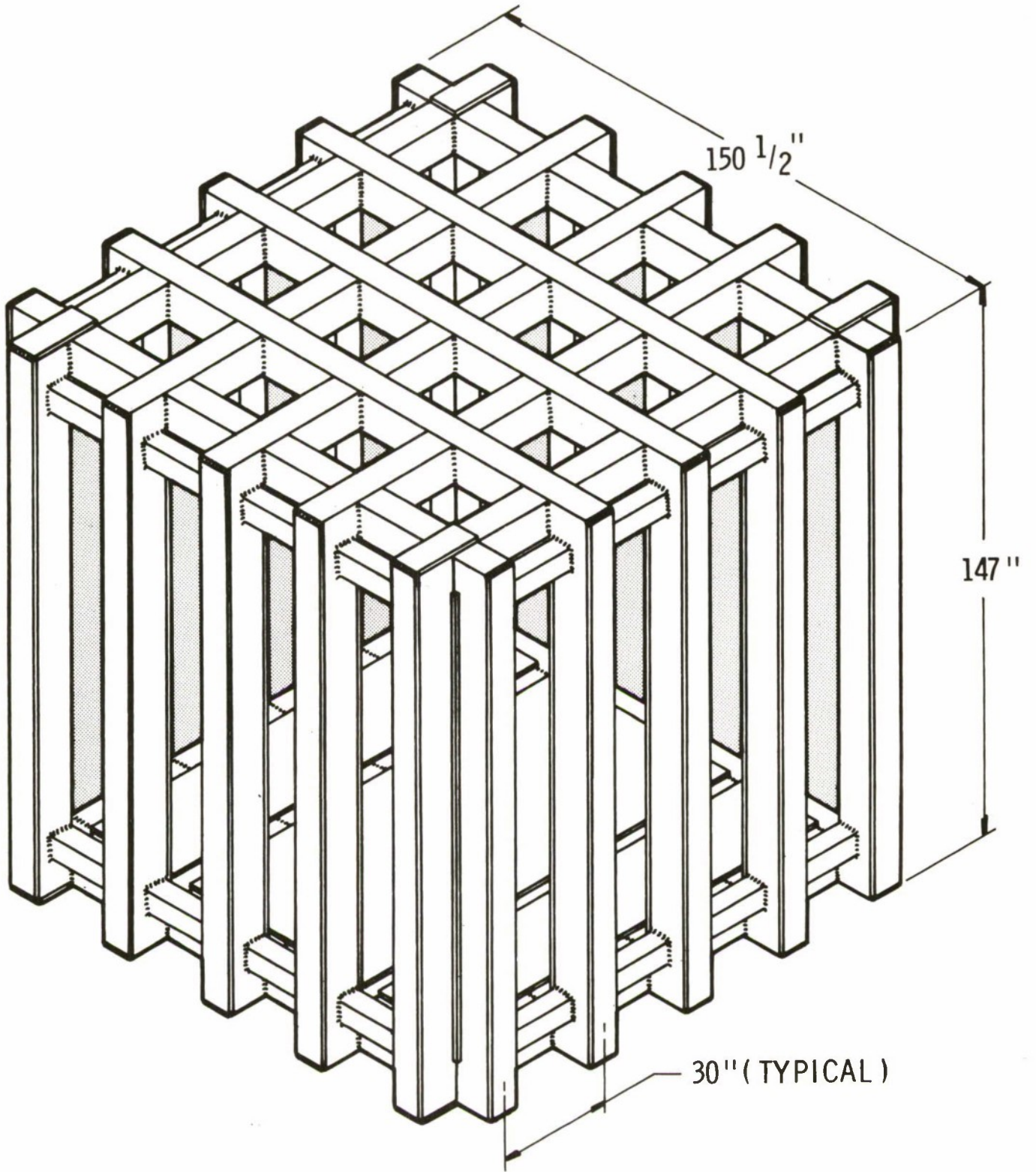


FIGURE 1. QUARTER-SCALE FRAME FOR RECTANGULAR BOX STRUCTURE

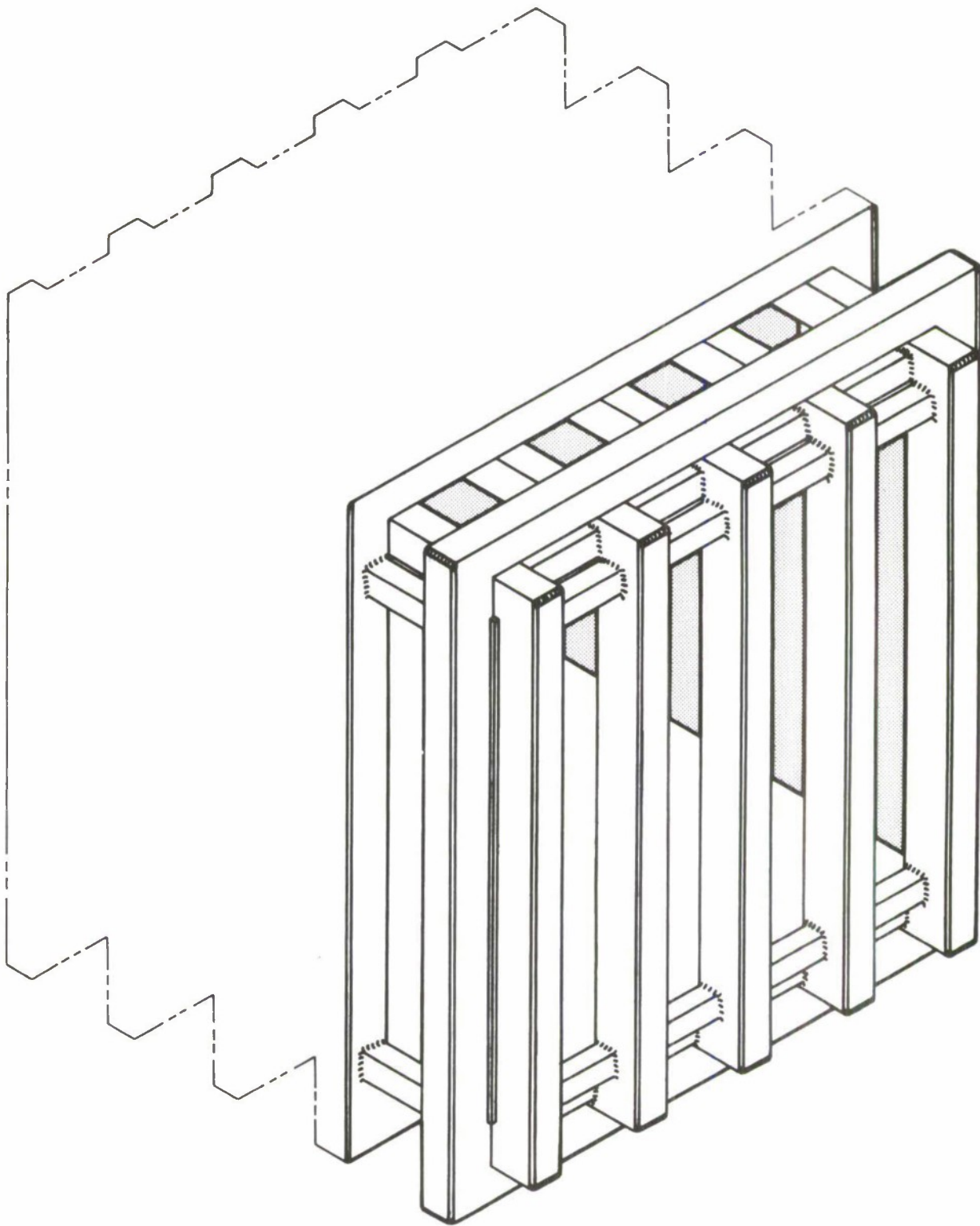


FIGURE 2. MODIFIED QUARTER-SCALE FRAME FOR RECTANGULAR BOX STRUCTURE

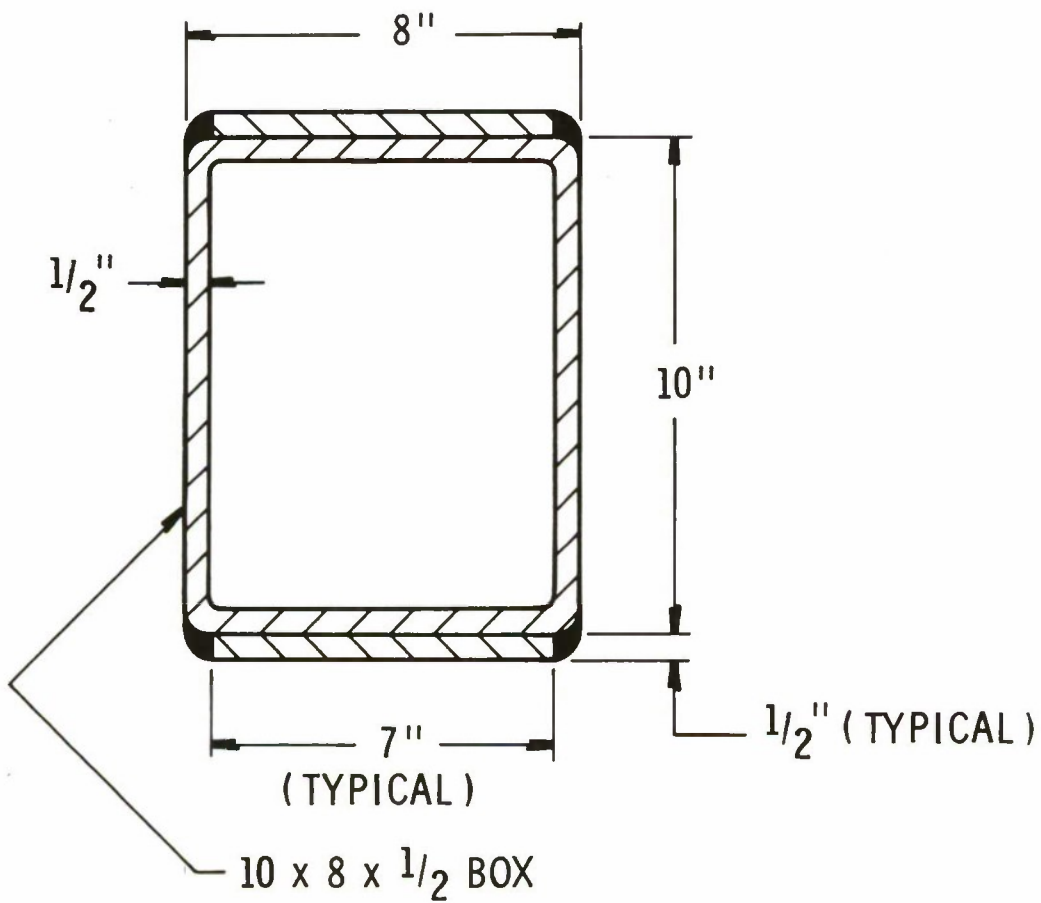
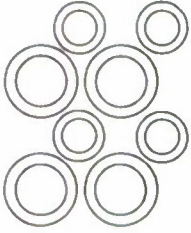


FIGURE 3. CROSS-SECTION OF FRAME VERTICAL MEMBERS IN QUARTER-SCALE BOX STRUCTURE

TABLE I. SUMMARY OF SWRI PANEL CONCEPTS

PANEL CONCEPT	PANEL CROSS-SECTION	ELEMENTS	FULL SCALE	1/4-SCALE	COMMENTS
1		ANGLES PLATES	3 1/2 x 3 1/2 x 1/2 9/16	7/8 x 7/8 x 1/8 9/64 10 Ga	<ul style="list-style-type: none"> <li>• Closed-spaced angles stop the fragments and absorb the reflected impulse.</li> <li>• Perforated plates withstand the quasi-static pressure, contacting and acting in series</li> </ul>
2		ANGLES PLATES	5 x 5 x 3/4 5/8	1 1/4 x 1 1/4 x 3/16 5/32 3/16	<ul style="list-style-type: none"> <li>• Angles and perforated plates are both required to stop fragments.</li> <li>• Angles are widely spaced and have no appreciable blast loading.</li> <li>• Perforated plates withstand both dynamic and quasi-static blast loading, acting in a series.</li> </ul>
3		PLATES	11/16	11/64 3/16 in	<ul style="list-style-type: none"> <li>• Plates designed initially to stop fragments.</li> <li>• Plates checked for response to dynamic and static blast loads; more than adequate for these loads.</li> </ul>
4		LARGE TUBES SMALL TUBES	5 OD, 3 1/2 ID 3 1/2 OD, 2 1/4 ID	1 1/4 OD, 7/8 ID 7/8 OD, 9/16 ID	<ul style="list-style-type: none"> <li>• Tubes designed to stop fragments.</li> <li>• Tubes checked for response to blast loads; more than adequate.</li> </ul>

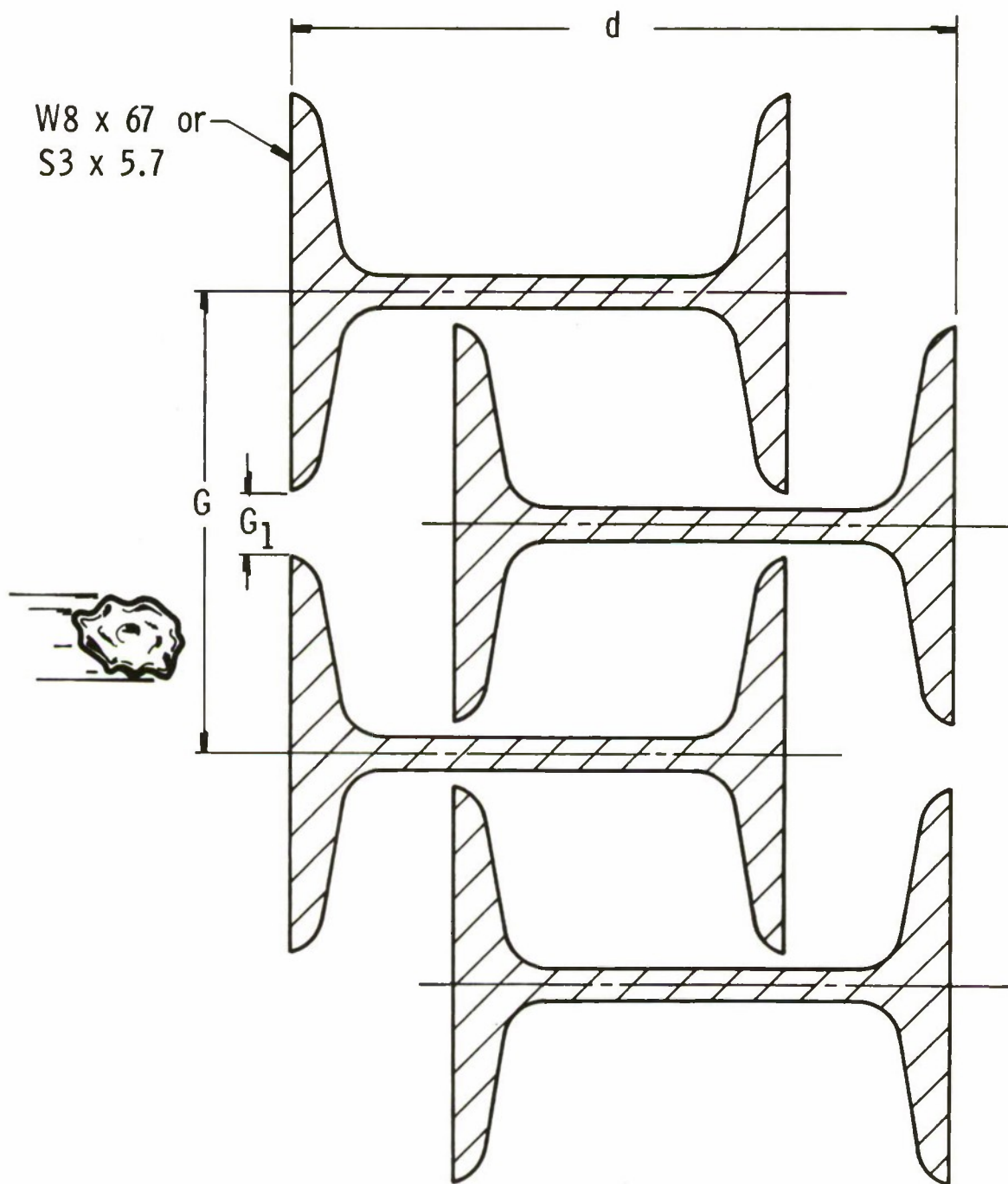


FIGURE 4. CROSS SECTION OF I-BEAM PANEL<sup>2</sup>

frame and held in place by simple attachments. This is possible because the I-beam type panels react the internal blast loads in a bending mode. On the other hand, panels with only membrane elements (SwRI Concept 3 of Table I) must be attached in a manner which will develop the in-plane loads in the membranes. Such an attachment is shown in Figure 5. A large amount of high quality welding is required for this type of attachment. Panels with both membrane plates and beams (SwRI Concepts 1 and 2) will require attachments less complicated than those for Concept 3 but more complicated than for the I-beam type panel.

Design for the rectangular box concepts continued through preparation of detailed design drawings. But, estimates of fabrication cost of these steel structures, having requirements for large amounts of high quality welding, were quite high, and the rectangular configuration was abandoned.

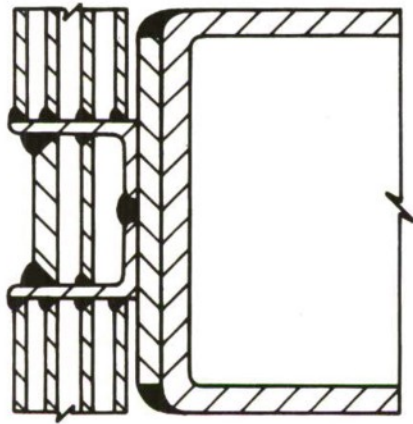
## 2. *Vertical Cylinder Concepts*

Because the rectangular configurations were too costly, a "brainstorming" session was conducted by Edgewood Arsenal Resident Laboratory (EARL) at NSTL,<sup>(6)</sup> to generate alternate concepts for steel suppressive structures. One concept advanced by D.M. Koger of EARL seemed quite attractive. It consisted of a vertical cylindrical structure with the cylindrical wall consisting of interlocking I-beams, supported externally by a series of spaced retaining rings. The roof was conceived as being made of interlocking I-beams or series of perforated plates, suitably supported and attached to the vertical I-beams.

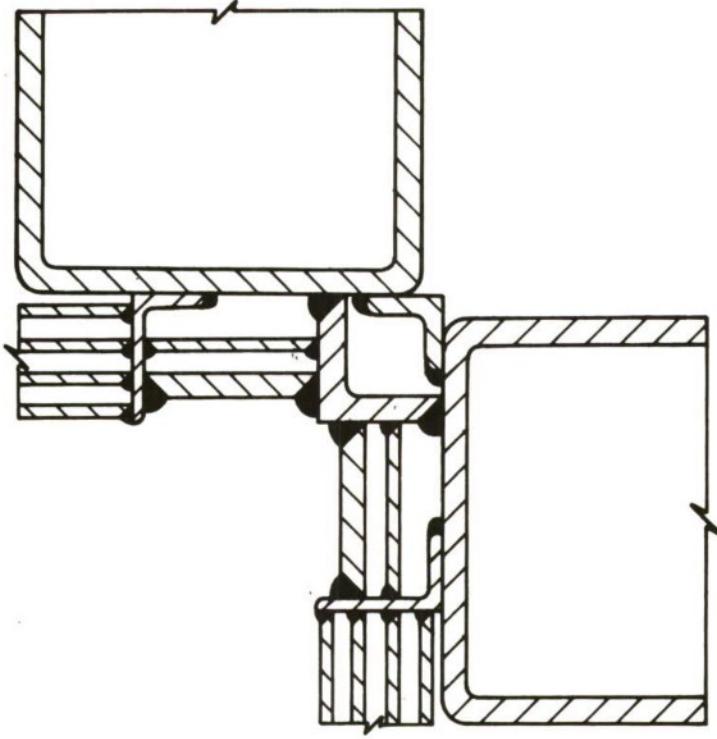
Following guidelines established at the NSTL brainstorming session, SwRI undertook a feasibility study of the cylindrical concept for the Category 1 suppressive shield. Its general configuration was to be:

- Vertical I-beams form the cylindrical portion of the structure with the beams chosen to defeat the fragment threat and to resist the internal blast loading between rings.
- Circumferential rings support the I-beams. They are sized to resist the internal overpressures applied to the I-beams in hoop tension.
- The top and foundation of the structure were undefined, but the top as well as the sides were to be fully vented.

The preliminary study revealed that a cylindrical I-beam concept was indeed feasible and estimates indicated that its weight would be less than half the weight of the rectangular box configuration and that it would be much less costly. This study resulted in the configuration shown in Figure 6. A membrane roof was initially chosen for this concept because, for the rectangular configuration, the membrane had been shown to be lightweight relative to other panel designs. Using a three-layer perforated membrane, a thickness of 3 in. was required to resist the internal pressure loads, and this thickness was also adequate to defeat the primary

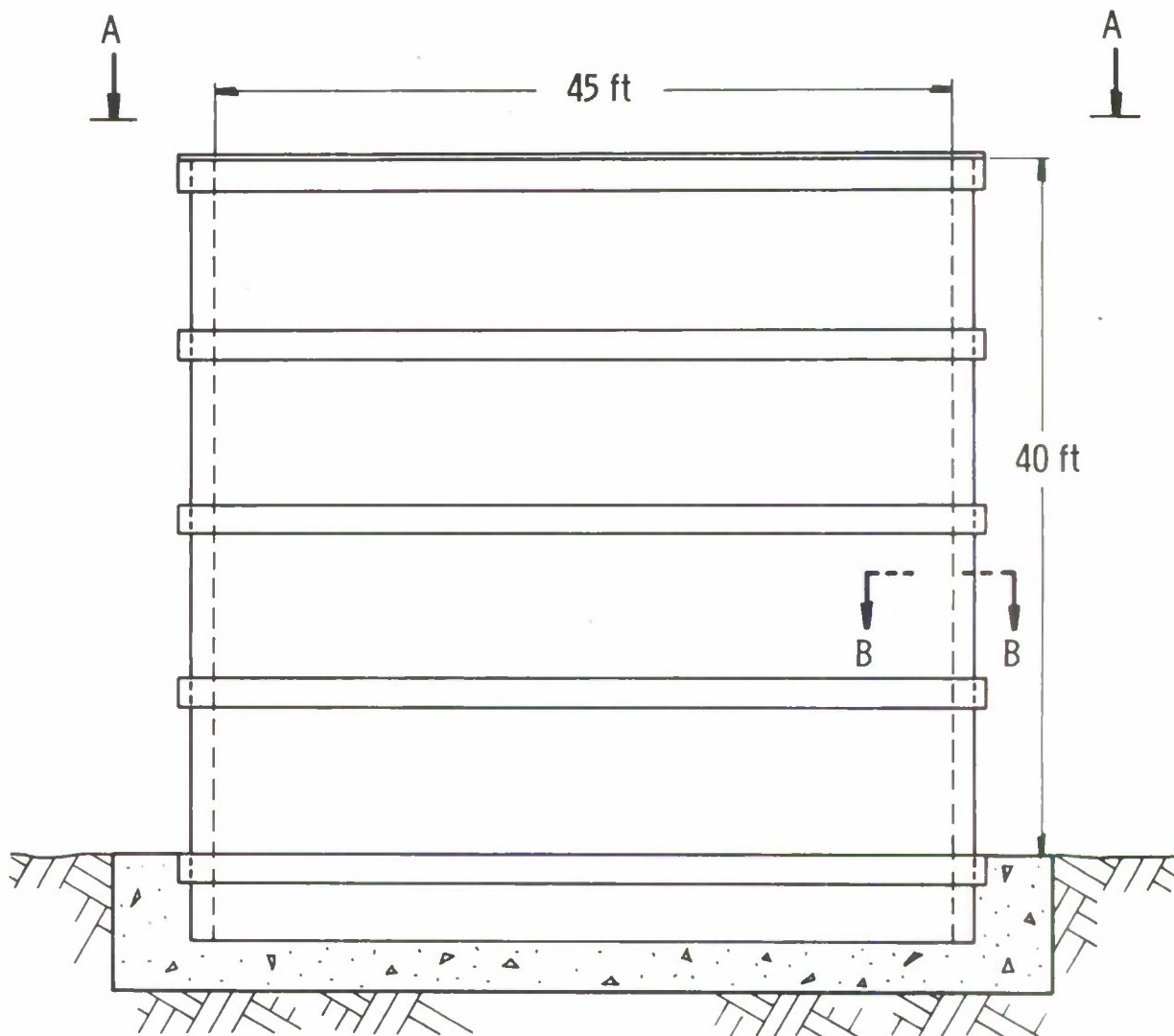


a. mid-wall connection



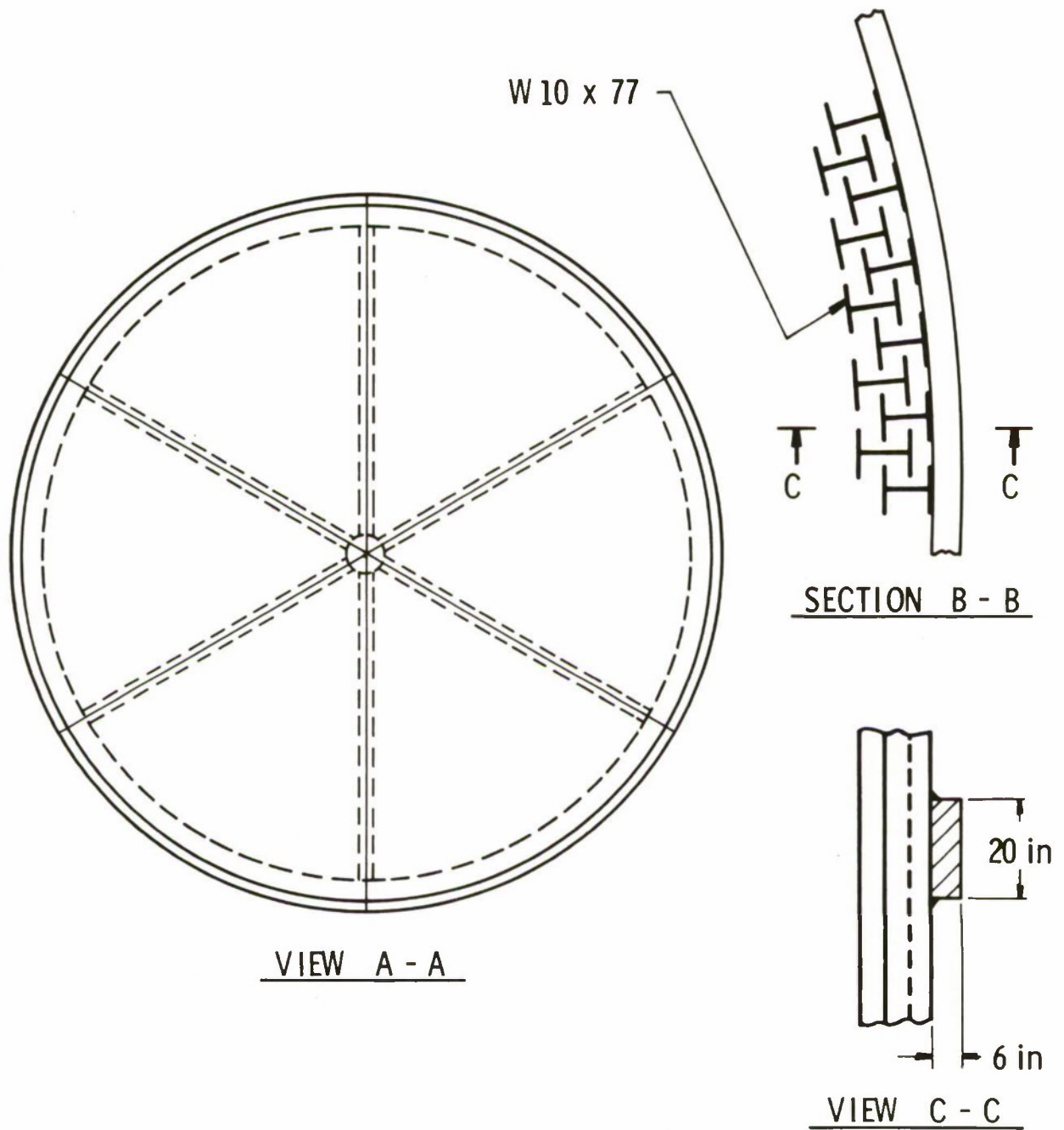
b. corner connection

FIGURE 5. TYPICAL PANEL INSTALLATION IN BOX STRUCTURE



( a ) Elevation

FIGURE 6. CYLINDRICAL CONCEPT



( b ) Planview and Details

FIGURE 6. CYLINDRICAL CONCEPT (Cont'd)

fragment. W10 X 77 beams were selected for the cylindrical portion of the structure. It has adequate bending strength and fragment stopping capability while giving a lower weight per unit length of cylinder (because of its greater flange width) than other beams investigated.

As shown in Figure 6, five equally spaced circumferential rings were used to react the internal pressure loads applied to the I-beams. The spacing is dependent upon beam strength, and it also controls the height of the opening into the structure. A door with a height of about 10 ft is made simply by cutting away the I-beams between two adjacent rings. With the 10-ft spacing, a preliminary analysis indicated that a cross-sectional area of 120 sq. in. per ring was required for the center rings and 60 sq. in. for the end rings on the cylinder. Alternately, the bottom ring could be omitted if the circumferential loads could be properly reached by the foundation. A reinforced concrete foundation was chosen as being a more suitable alternative for the structure than attempting to design one of steel.

### C. Alternate Cylinder and Roof Configurations

Following the feasibility study, SwRI undertook a more thorough design analysis of a suitable cylindrical concept for the Category 1 prototype and one-quarter scale test model. Initial guidelines were the same as for the feasibility study except that additional cylindrical concepts were to be evaluated, such as concentric perforated cylinders. A more thorough study of roof designs was also undertaken to find suitable alternative to the membrane.

Four roof concepts were investigated as well as the two concepts considered for the cylindrical portion of the structure. The six concepts include:

#### Cylinders:

- I-beam cylinder
- concentric perforated cylinders

#### Roof concepts:

- membrane roof
- lifting or pop-up roof
- I-beam roof
- double-dome roof

They are discussed in detail in the following paragraphs.

## 1. I-Beam Cylinder

The I-beam cylindrical portion of the structure remained much the same as that developed in the feasibility study (refer to Figure 6). Further analysis of the beam and ring response lead to the use of W8 X 67 beams in place of the W10 X 77 beams initially recommended, and to an increase in the ring cross-sectional area from 120 sq. in. to 140 sq. inches. These analyses were performed using the computer code DANAX4A developed at SwRI, and they are described more fully in Appendix B. The W8 X 67 develops the lowest shearing stress at the foundation (full lateral and rotational constraint assumed) and provides greater fragment stopping capability because of slightly greater flange thickness (refer to Appendix C for a discussion of the fragment requirements of the shield).

Even with the W8 X 67 beams, the analysis predicts high shearing stresses in the web which exceed the minimum expected ultimate shearing stress of the material. For W8 X 67, W10 X 77 and S3 X 5.7 (one-quarter-scale) beams, the computed shearing stresses in the Category 1 shield were:

$$\text{W8 X 67: } \sigma_s = 47.1 \text{ ksi}$$

$$\text{W10 X 77: } \sigma_s = 61.0 \text{ ksi}$$

$$\text{S3 X 5.7: } \sigma_s = 42.4 \text{ ksi}$$

An additional calculation was made for the S3 X 5.7 beam corresponding to the maximum loading conditions which existed in the sub-scale venting tests of 1-1/2 foot cubes<sup>12</sup>. This calculation produced a maximum shearing stress of

$$\sigma_s = 41.4 \text{ ksi}$$

For A 36 steel the ultimate shearing stress can be estimated as 60% of ultimate tensile stress which has a range of 58 Ksi to 83 Ksi. This gives a range for the ultimate allowable shearing stress of the material:

$$F_{su} = 34.8 \text{ ksi to } 49.8 \text{ ksi}$$

Thus, except for the W10 X 77 beam which was discarded, all of the values computed fall within the range of the ultimate stress. However, all of the stresses are higher than desired. One way to reduce the stress is to design for simple support at the foundation. For example, if this can be achieved, then the maximum shearing stress in the W8 X 67 beam is reduced to 33.5 ksi at the foundation. However, the shearing stress at the rings, which is 38.9 ksi, now predominates. Because the shearing stress in the S3 X 5.7 beams predicted for the 1/4-scale model and for the 1/16-scale venting tests are about the same, and because no failure occurred in the 1/16-scale venting test, we feel that the use of the S3 X 5.7 beam in the 1/4-scale model is acceptable. Careful measurements should be made on the 1/4-scale model, and perhaps

additional scale-model testing conducted, to better define the shearing stresses which exist in the I-beam under dynamic loads and to establish a suitable criteria for failure. These data are needed before the W8 X 67 beams can be used with confidence in the prototype structure.

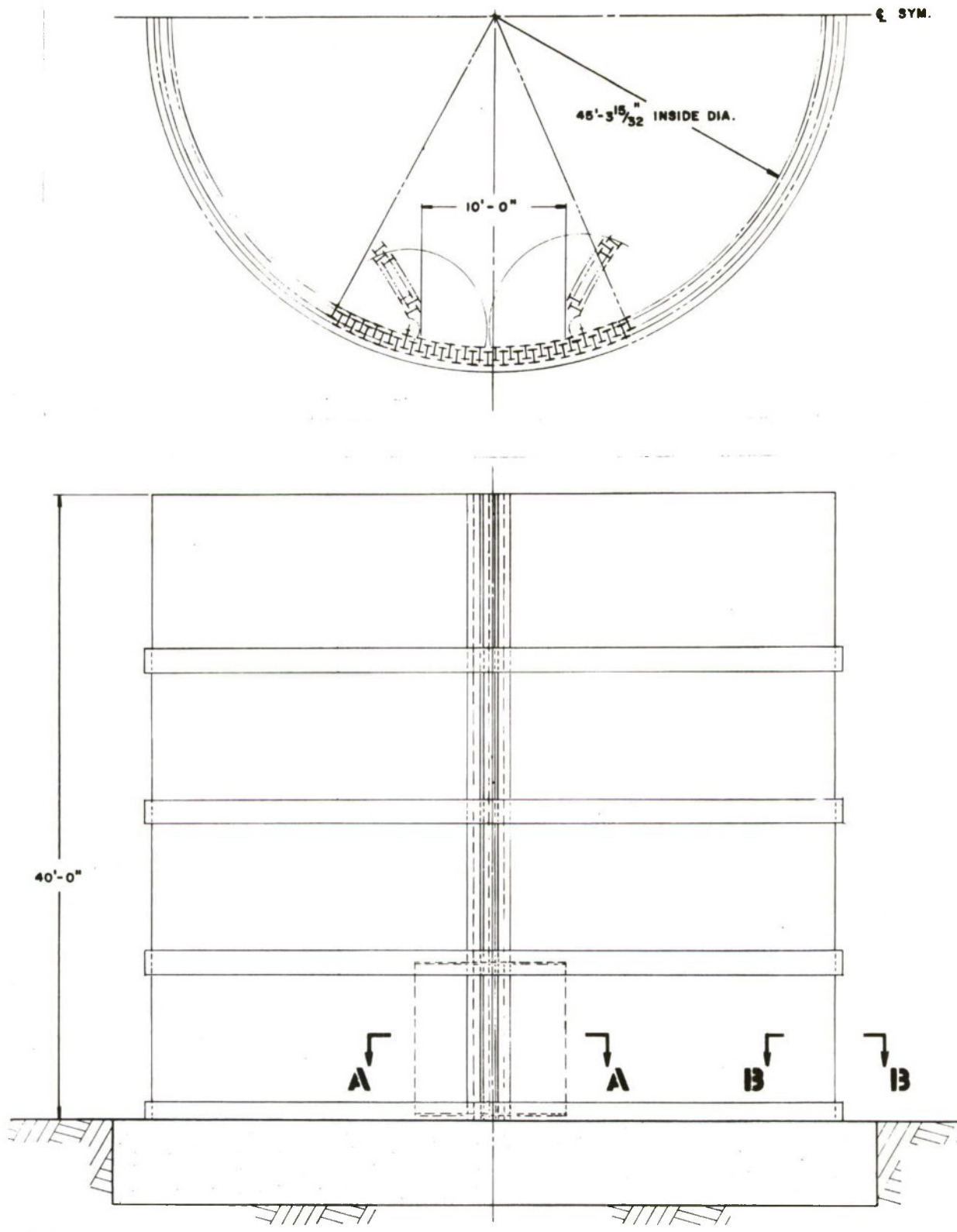
In addition to the beam selection and ring sizing for the cylindrical portion of the structure, a 10 X 10 ft access door was designed for the cylinder, and other general design details were completed. Drawings of this configuration are included as Figure 7.

Design of the foundation in 1/4-scale was completed by the Corps of Engineers, Huntsville, Alabama. Details of the foundation are given in COE drawing (entitled "Suppressive Shield Quarter Scale Model Category I") and are not shown here. It is constructed of reinforced concrete, and the cylindrical cage is bolted to the foundation through flange fittings on the ends of the beams. This attachment closely approximates "fixed" end conditions. As mentioned earlier, we recommend a simply supported end condition for the I-beams at the foundation based on current knowledge. Results of the 1/4-scale testing will either confirm the adequacy of the existing design or dictate the revisions that need to be made.

## 2. *Perforated Cylinder*

Another concept studied for the cylindrical portion of the shield involves the use of concentric cylinders of perforated plate. As for the SwRl panels (Table 1), additional steel thickness above that required to withstand the blast loading is needed to contain the primary fragment. Alternatives are to use multiple layers of plate (concentric cylinders) or to place additional material inside the cylinders for fragment suppression. The configuration chosen as being the least expensive was to use two perforated concentric cylinders, which are designed to withstand the blast loading only, and to place stacked angles inside the cylinders for additional fragment suppression. This configuration is shown in Figure 8.

Access to the structure through the thin wall cylinder is more difficult to provide than for the I-beam cylinder. In the I-beam arrangement, the circumferential rings react the pressure loads in tension, and the beams must only transfer pressure loads to the rings in bending. Thus, the I-beams can be cut without damaging the integrity of the structure. In the thin wall cylinders, however, high circumferential tension loads are developed in the walls of the cylinder, and when the cylinders are cut, provisions must be made to transfer these loads across or around the opening. The most direct approach is to design the door to transmit the loads across the openings rather than to design a frame to transmit the loads around the opening. This approach was used for this concept, and design details are included in Figure 9. While door frames can be designed to transfer loads around the opening, this is a particularly difficult problem for structures undergoing large plastic deformations, and the design and analysis effort required for this approach was not warranted in this study. Doors designed for similar types of structures undergoing only elastic deformations would not be acceptable.



(a) Overall view

FIGURE 7. DOOR AND ASSEMBLY DETAILS OF THE I-BEAM CYLINDER

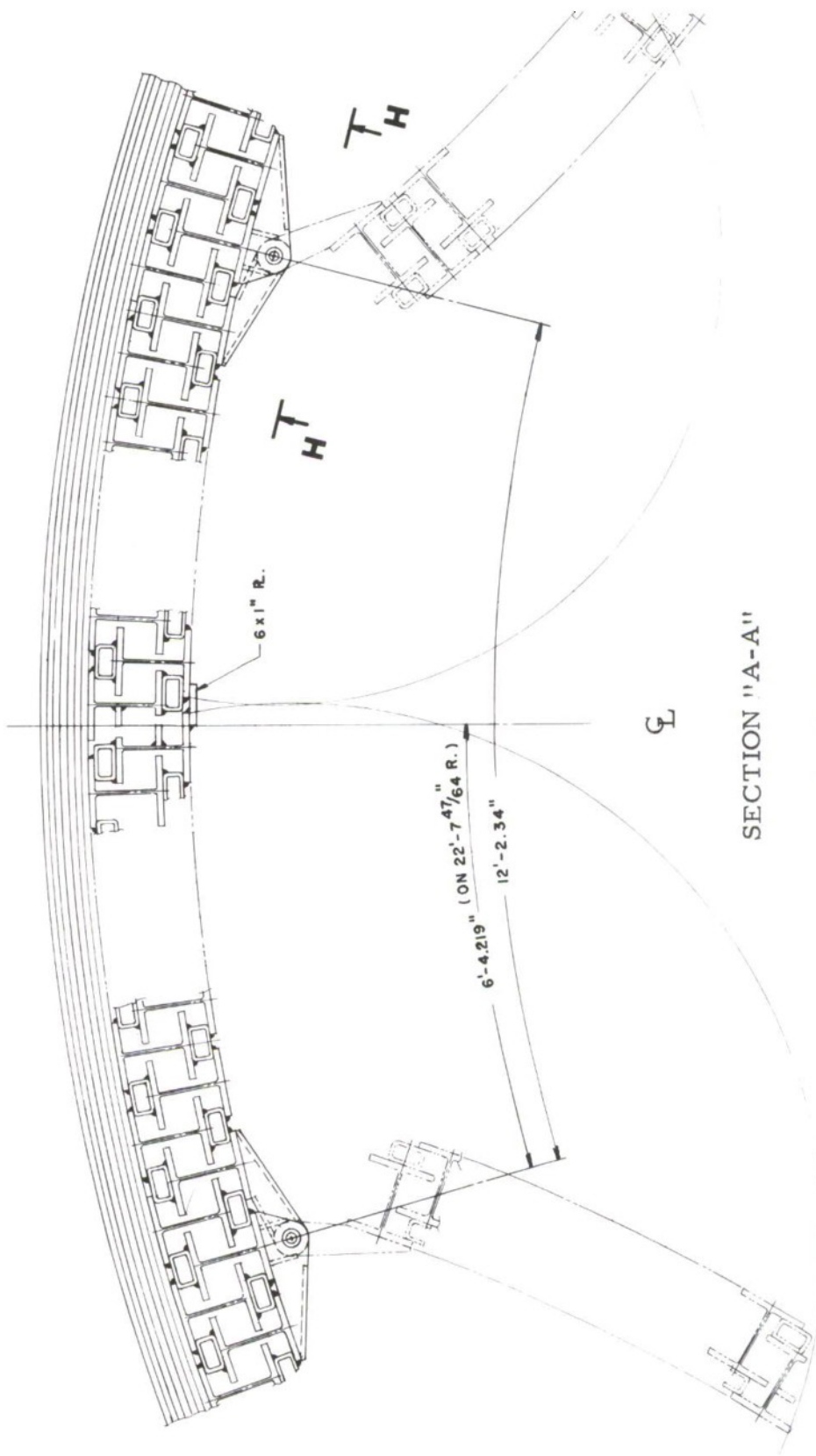
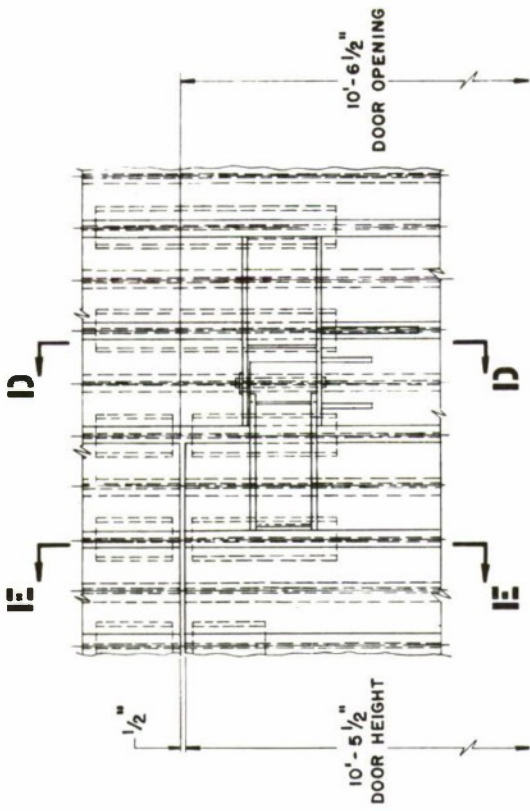
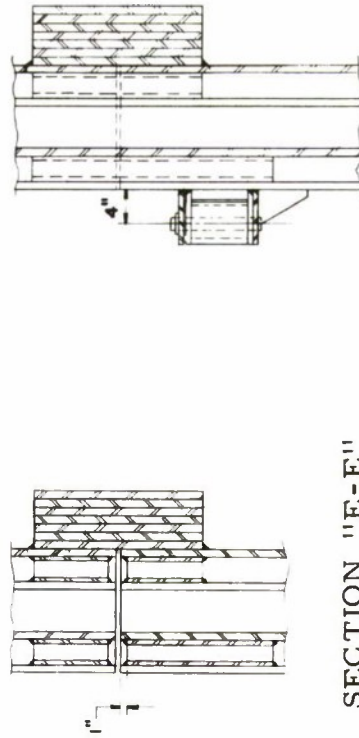


FIGURE 7. DOOR AND ASSEMBLY DETAILS OF THE I-BEAM CYLINDER (Cont'd)

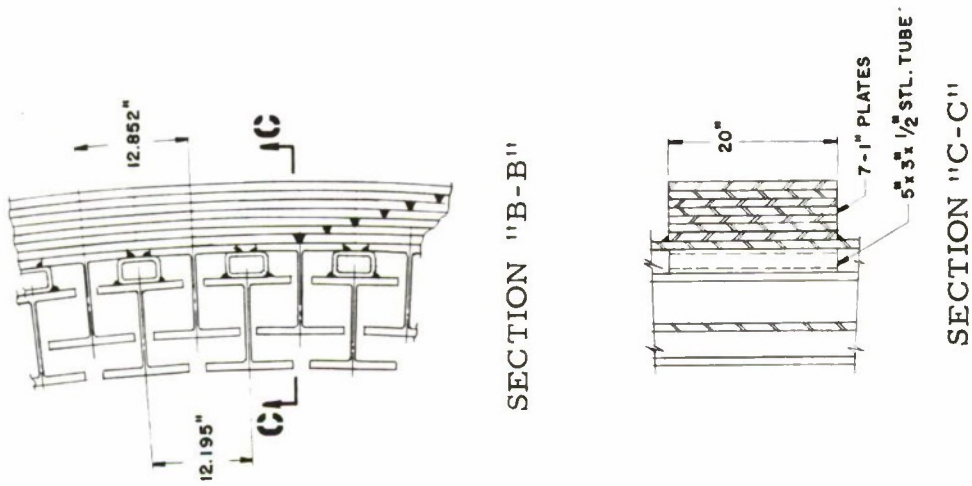


VIEW "H-H"



SECTION "E-E"

SECTION "D-D"



SECTION "B-B"

SECTION "C-C"

(c) Wall and hinge details

FIGURE 7. DOOR AND ASSEMBLY DETAILS OF THE I-BEAM CYLINDER (Cont'd)

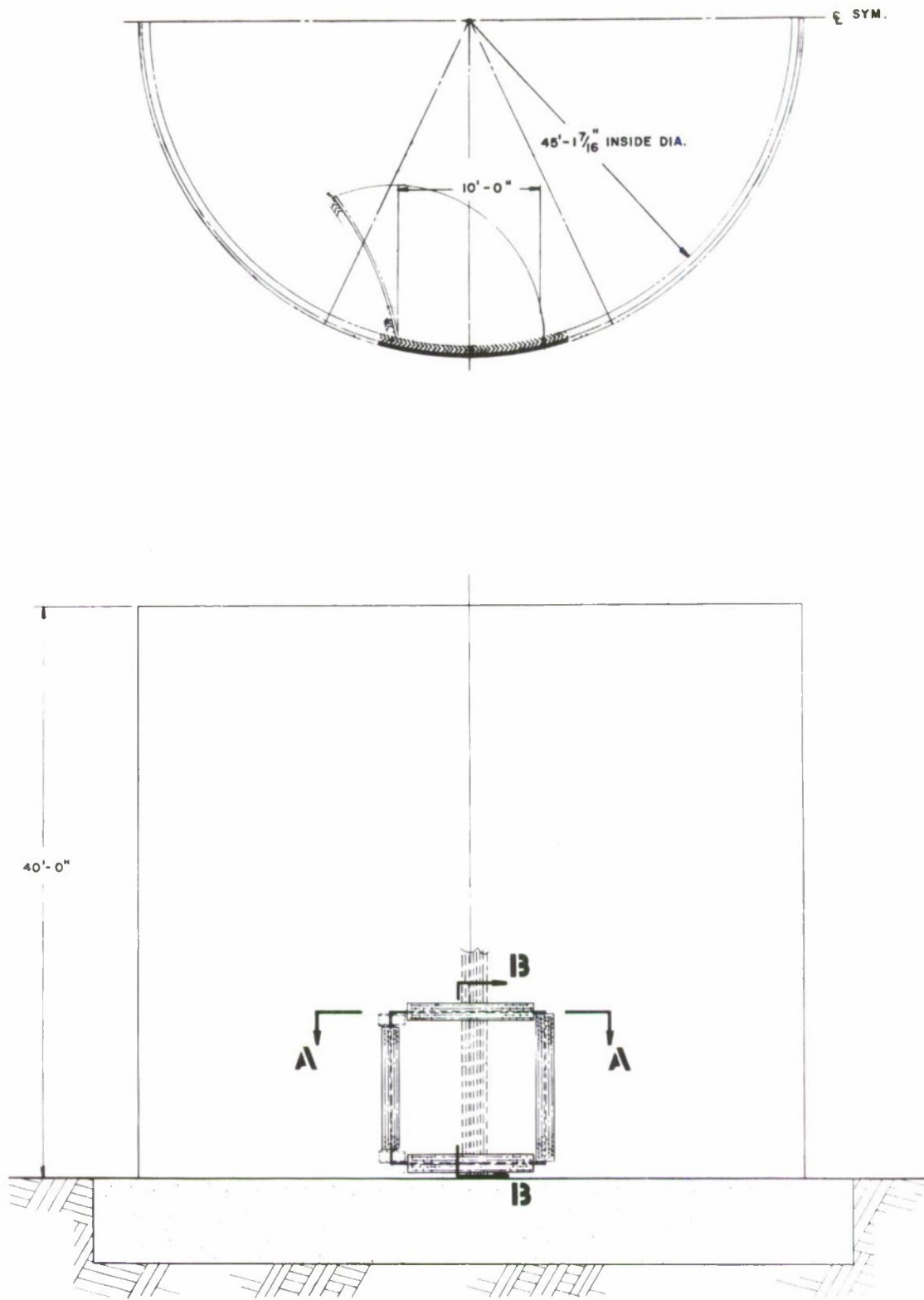
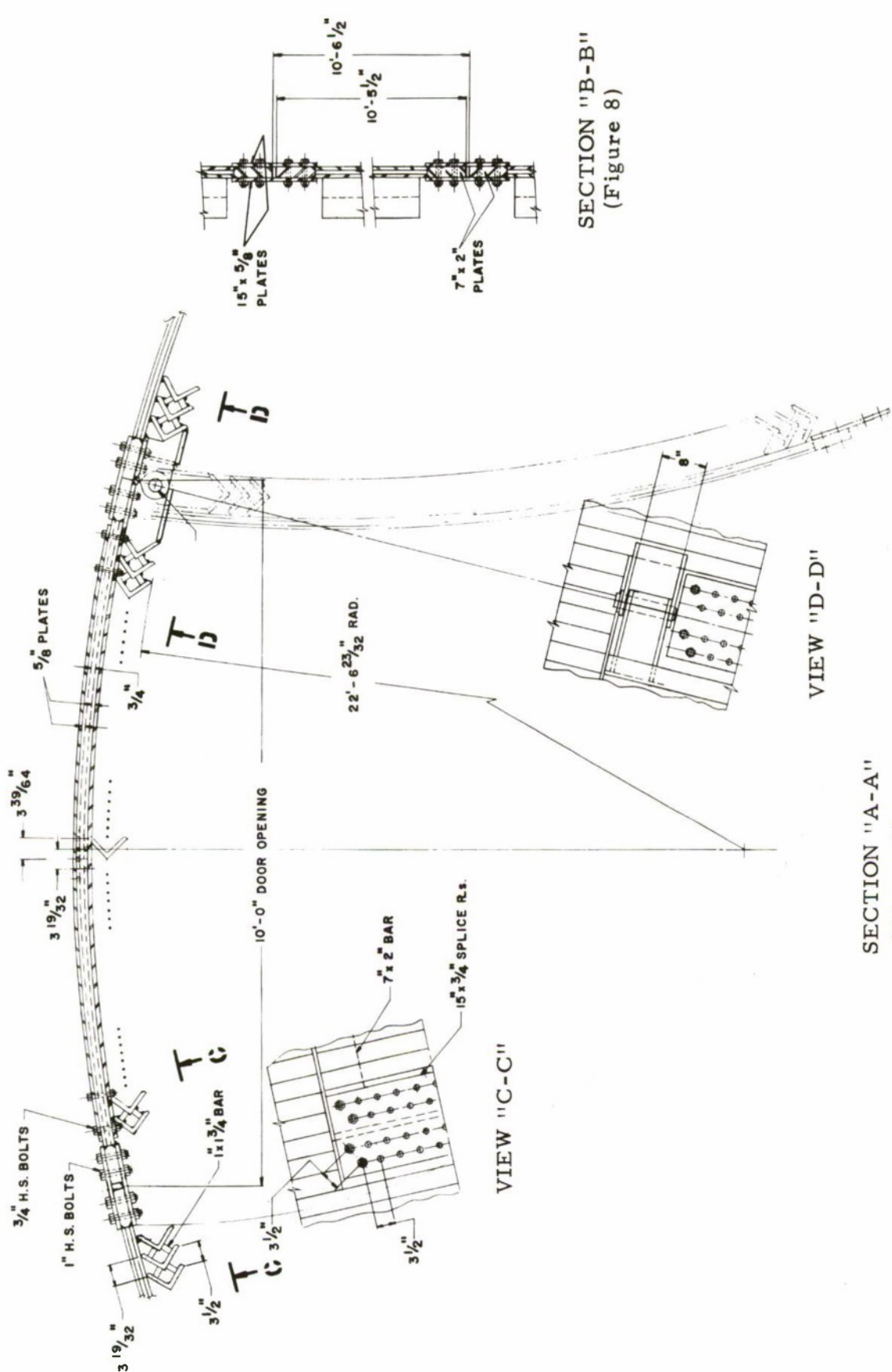


FIGURE 8. PERFORATED CYLINDER



SECTION "B-B"  
(Figure 8)

SECTION "A-A"  
(Figure 8)

VIEW "D-D"

FIGURE 9. DOOR DETAILS FOR PERFORATED CYLINDER

Steel fabricators,\* who reviewed the drawings of both the I-beam cylinder and the perforated cylinder, expressed the opinion (without a detailed cost estimate) that the I-beam concept would be cheaper to fabricate and erect than the perforated cylinder concept. As a result of these contacts, the perforated cylinder was eliminated from further consideration, in favor of the I-beam design.

### 3. *Membrane Roof*

The membrane roof consists of three layers of perforated plate, each approximately 1 in. in thickness, with a light internal I-beam framework to support the roof and aid in assembly (see Figure 6). Design analyses indicated that the cylinder would not develop the high in-plane loads from the membrane but would deflect inward, allowing the membrane to deform with reduced stretching. This will also induce buckling at the edge of the membrane, as well as large rotations in the membrane at the support. Furthermore, it was not feasible to design a top ring stiff enough to react the membrane forces without buckling, so an attempt was made to support the membrane in such a way that rotations could be tolerated.

The final design for the junction between the membrane roof and the vertical cylinder is shown in Figure 10. Even though we felt that this design could tolerate rotations, buckling still presented potential problems which only a testing program could adequately resolve. If this design had been pursued, scale-model testing could have been used conveniently to optimize the design. However, conversations with manufacturers who reviewed the drawings indicated that rolling the edge members with the double curvature would be very costly. Thus, even though the membrane roof was attractive from the standpoint of weight, the expense associated with the attachment to the cylindrical portion of the structure, plus the uncertainty which would need to be resolved by scale-model testing (even before the 1/4-scale test fixture was designed) caused us to discard this concept.

### 4. *Lifting Top*

Because of the difficulty experienced in joining the membrane roof to the cylinder, a lifting or "pop-up" top was considered. The lift imparted to a roof by the initial impulse was checked and found to be reasonable. For example, the impulse from the initial blast wave will cause a roof weighing 350 tons to rise about 10 ft. This was felt to be acceptable for a 45-ft diameter roof, i.e., the roof would not be considered a fragment since it would simply settle back into the cylinder after the explosion. However, the quasi-static pressure also has a contribution to the roof velocity, and an incremental solution was required which accounted for the increase in venting area as the roof rises from the cylindrical portion of the structure. These calculations were performed, and it was found that, with the contribution due to the quasi-static pressure, the 350-ton roof would rise more than 120 ft above its initial position. These calculations were made in the absence of any constraint which might be applied to limit the rise of the roof. Since this distance was clearly unacceptable, means of restraining the roof were pursued so that its height of rise could be reduced to

\*Pittsburgh Des Moines Steel Co., Mosher Steel Co., and Trinity Industries.

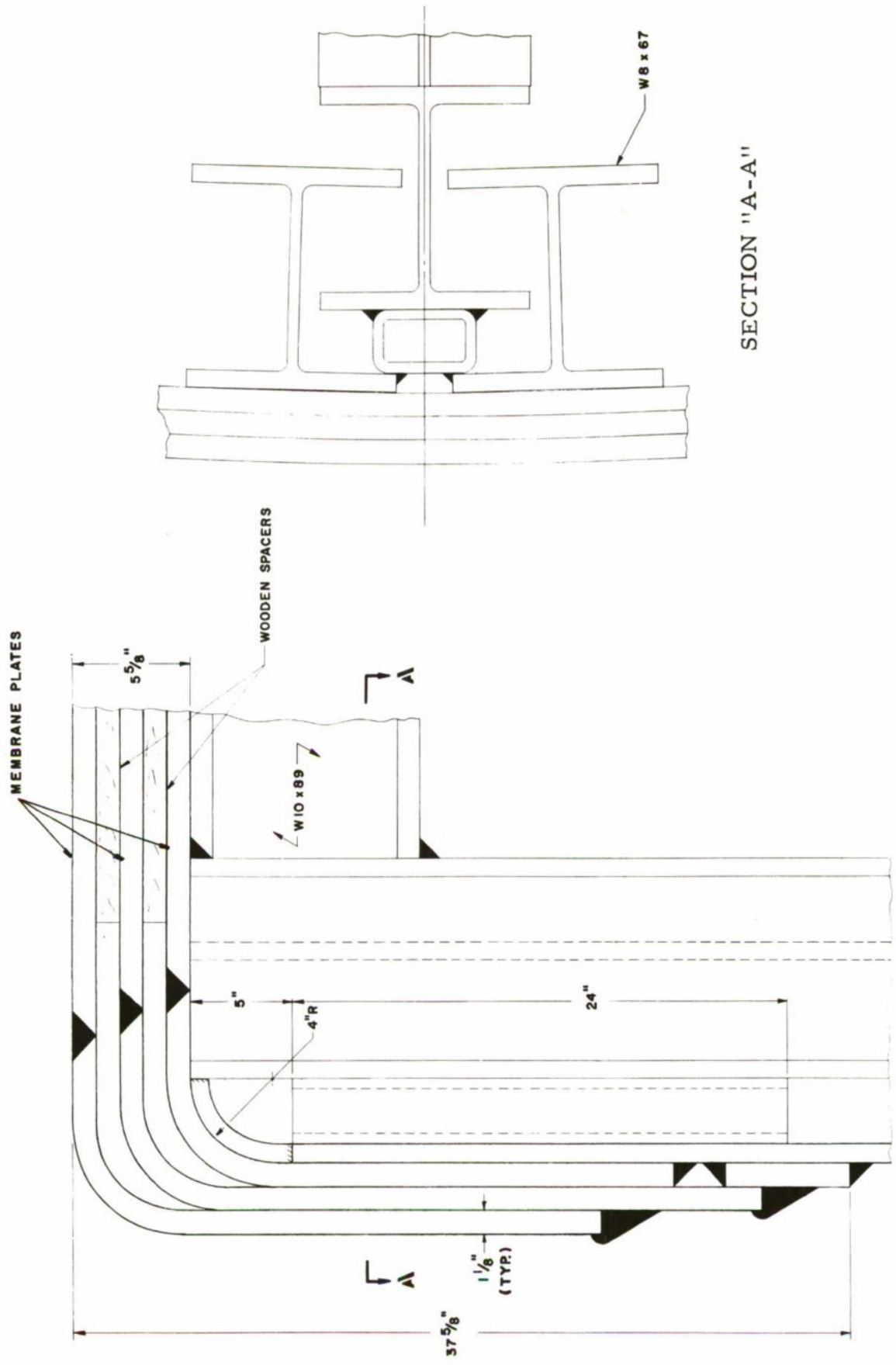


FIGURE 10. ATTACHMENT OF MEMBRANE ROOF TO I-BEAM CYLINDER

acceptable values. Thus, a series of calculations was performed using constant constraint forces such as might be provided by a series of yielding rods. Results of these calculations are shown graphically in Figure 11 for three different roof weights. The corresponding quasi-static pressure decay is given in Figure 12. As indicated earlier, these pressures were computed on the basis of an ever-increasing vent area as the roof rises from the cylinder. The decay rate is obviously a function of both roof weight and the restraining force. For example, the unrestrained 300 ton roof produces a slower venting time for the quasi-static pressure than does a 100-ton roof which is lightly constrained.

The results in Figure 11 show that large restraining forces coupled with heavy roofs must be used to limit the rise of the roof to reasonable values. Furthermore, the permissible rise of the roof is limited by the mechanism used to apply the constraint. For this application, the most suitable approach appeared to be the use of yield rods placed around the circumference of the roof at some convenient spacing. Because a 10-ft door opening is desirable, the spacing was set at a 10-ft minimum which gives approximately 15 yielding rods. If the stretching of the rods is limited to 10% ( $\epsilon_u/\epsilon_y = 50$ ), the allowable roof rise is limited to 4 ft. From Figure 11 it is found that a constant restraining force of 19 million pounds must be applied to a 300-ton roof to limit the height of rise to this value. If yielding of the rods occurs at 40,000 psi, then 6.3-in.-diameter rods are needed to develop the necessary restraining force. Tie-down problems associated with rods this large would be formidable and, with cross-sectional areas this large, less confidence can be placed in the rods' strength at these high elongations.

Although this concept was not completely dismissed (it still seemed a possible solution), other concepts were investigated in the hope of finding a less complicated and less costly solution. Another disadvantage to this concept would be the difficulties associated with the 1/4-scale testing. Provisions would be required to catch the roof during its rise to prevent damage to the roof and to the cylindrical portion of the shield, since repetitive firings are required. Also, the rods would have to be retensioned or replaced between tests.

### 5. *I-Beam Roof*

Another concept was studied which was basically an application of the interlocking I-beams used in the cylindrical portion of the structure, to the roof as well. In this concept beams, identical to those used in the cylinder, would be supported by larger beams radially placed like spokes from a central hub. The areas between the larger beams are filled by the interlaced W8 X 67 beams in a circumferential pattern. A sketch of this configuration is shown in Figure 13. Blast loading on the smaller I-beams is transferred to the large radial beams, which then transfer the loads, primarily in bending, to the walls of the cylinder. For the layout in Figure 13 the largest commercially available beams, W14 X 730, were used for the spokes. An analysis of this configuration was performed using an SwRI computer program, DANAX4A, with the details given in Section VI. The results showed that the velocity of the roof was still increasing as center deflections exceeded 14 ft. Thus, a larger beam is required for the spoke member, and this beam would have to be specially fabricated. Because built-up members are expensive to fabricate, this concept was abandoned.

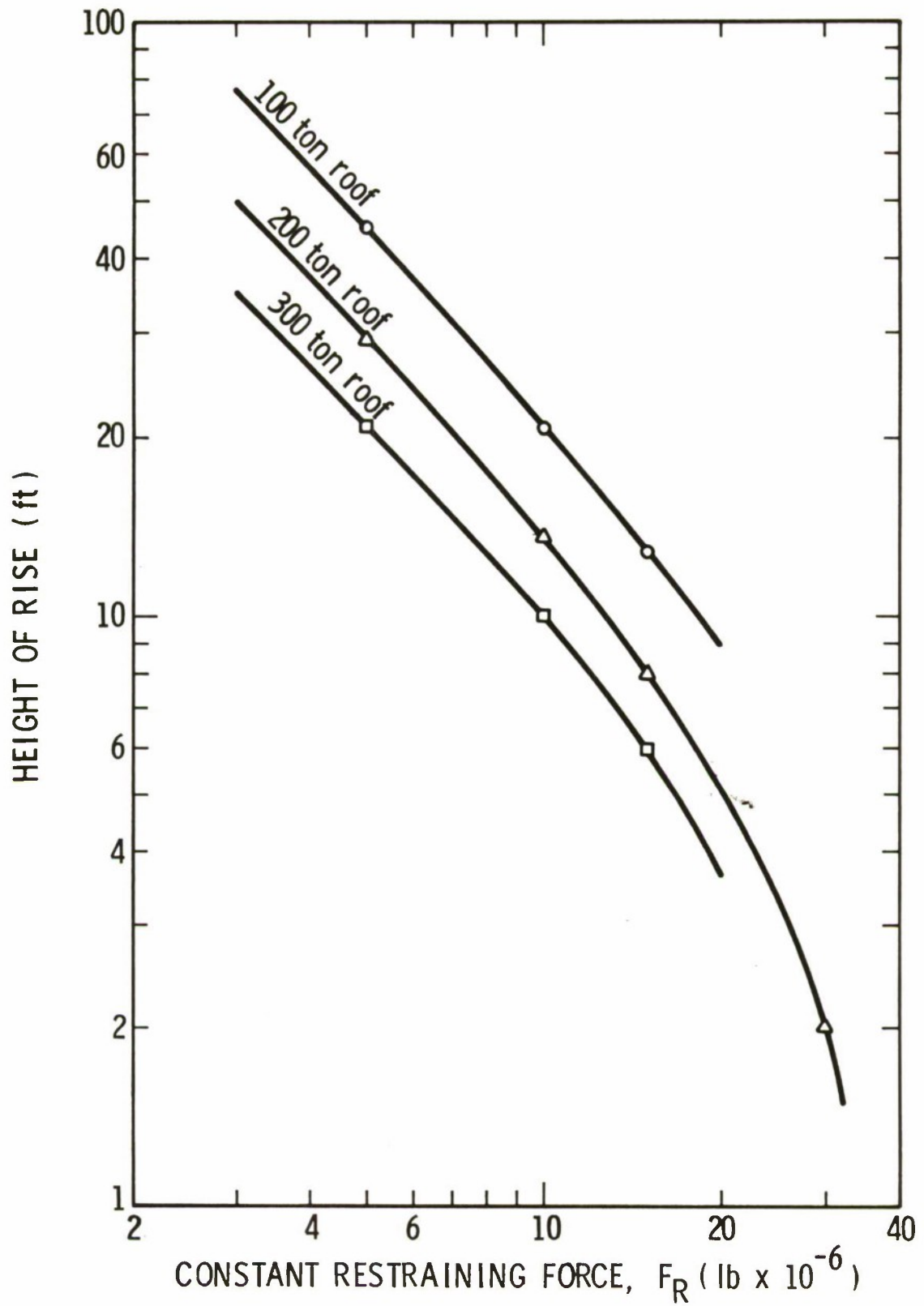


FIGURE 11. HEIGHT OF RISE OF RESTRAINED ROOF

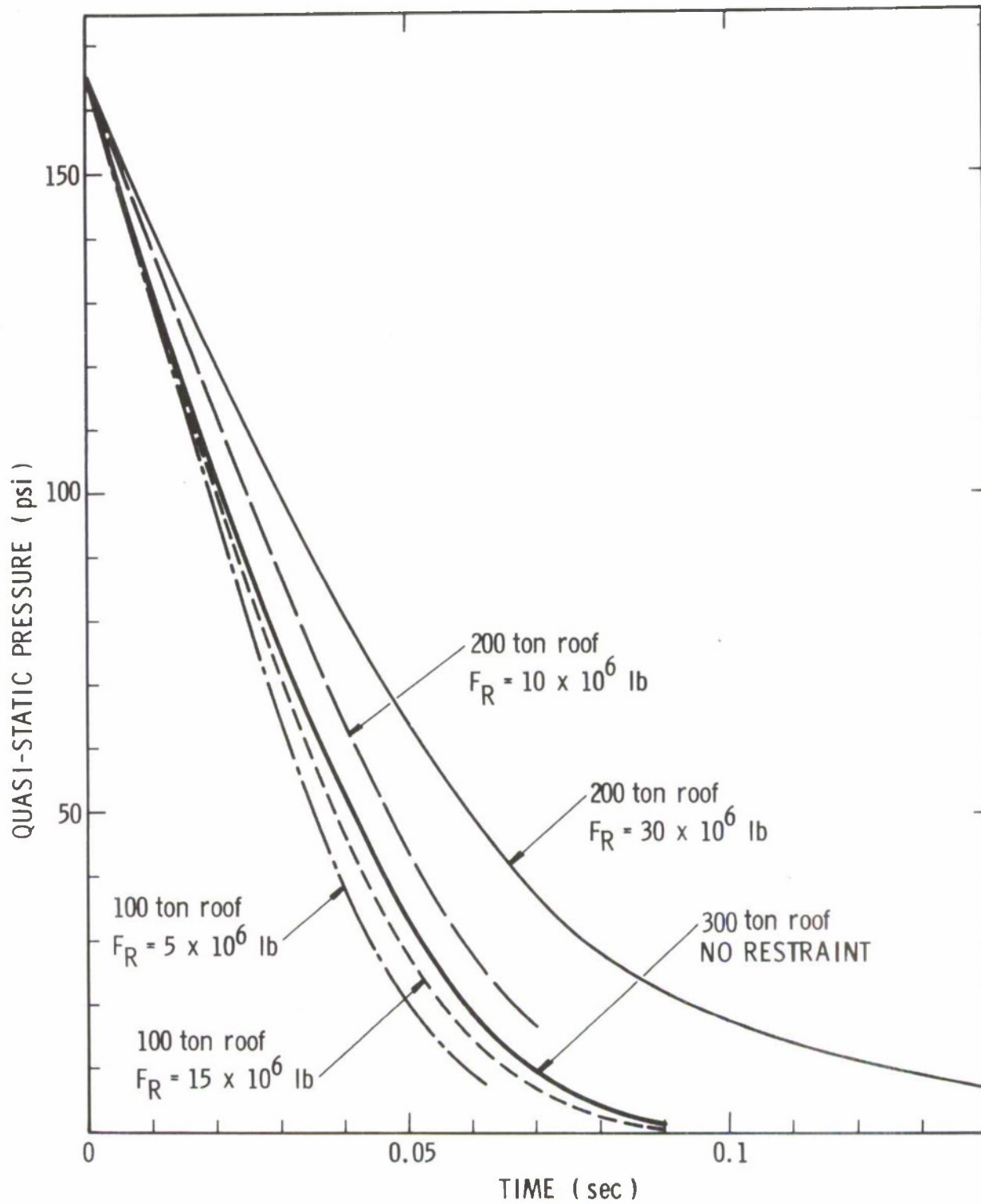
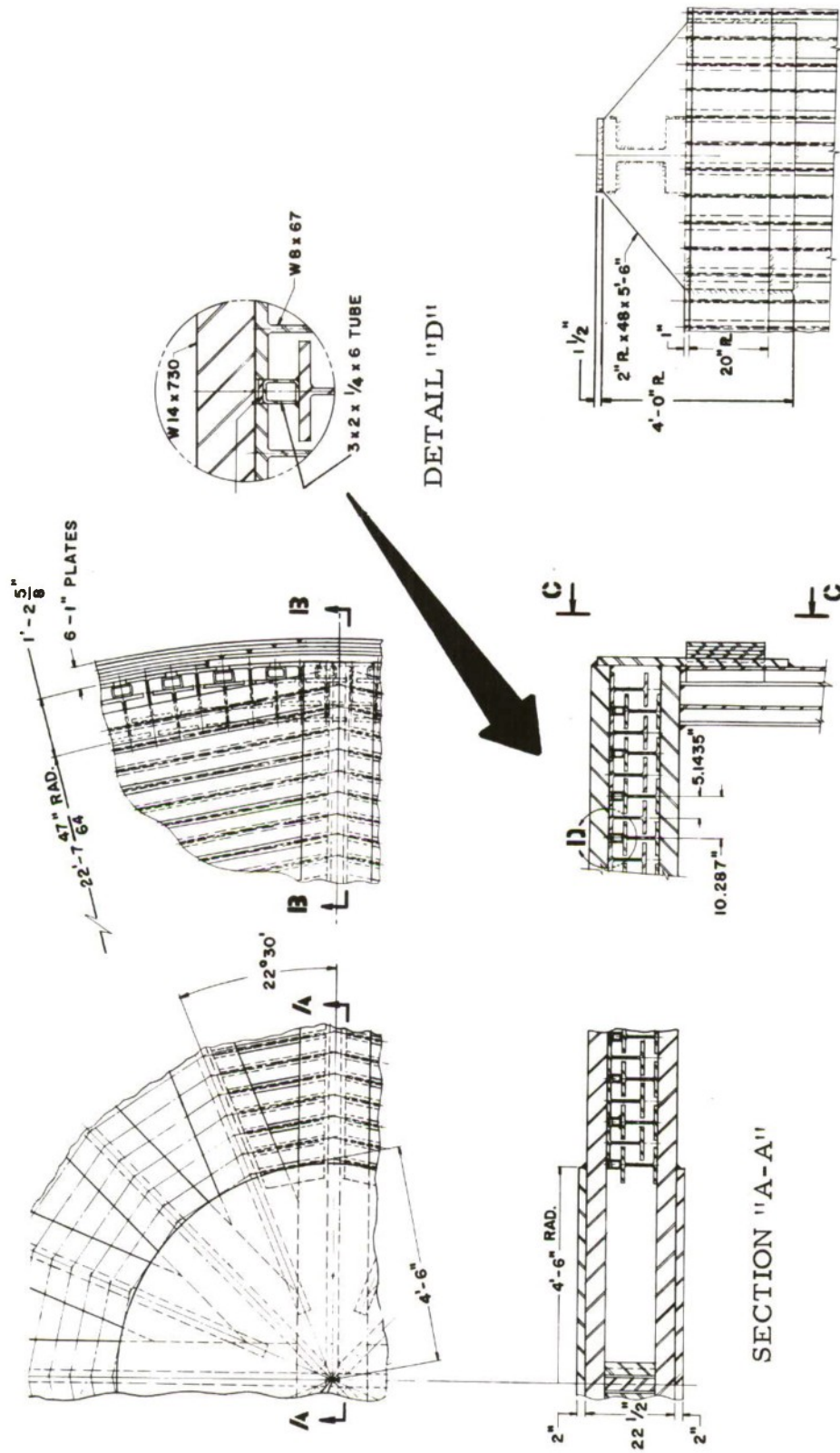


FIGURE 12. QUASI-STATIC PRESSURE FOR LIFTING ROOF DESIGN



SECTION "B-B"

VIEW "C-C"

FIGURE 13. I-BEAM ROOF CONCEPT

## 6. Double-Dome Roof

The roof concepts already described were developed when it was felt that a vented roof structure was a desirable goal for the suppressive shield; however, after results for the 1/16-scale venting tests<sup>(7)</sup> showed that the peak quasi-static pressure was not significantly affected by the venting area (over the range of venting ratios being considered for the suppressive shields), the requirement for a vented roof was relaxed. So, whereas in the past it had seemed unpractical to use a multi-layered vented dome roof, a single dome, or perhaps two widely spaced domes without holes, now seemed much more practical.

An initial configuration utilized two hemispherical domes separated by 10 ft of sodium silicate foam, as shown in Figure 14. In this concept the outer dome is designed for the blast loading, while the inner dome and foam layer were designed to defeat the fragment threat. Of course, the inner dome provides support for the foam and a smooth inner surface for the shield.

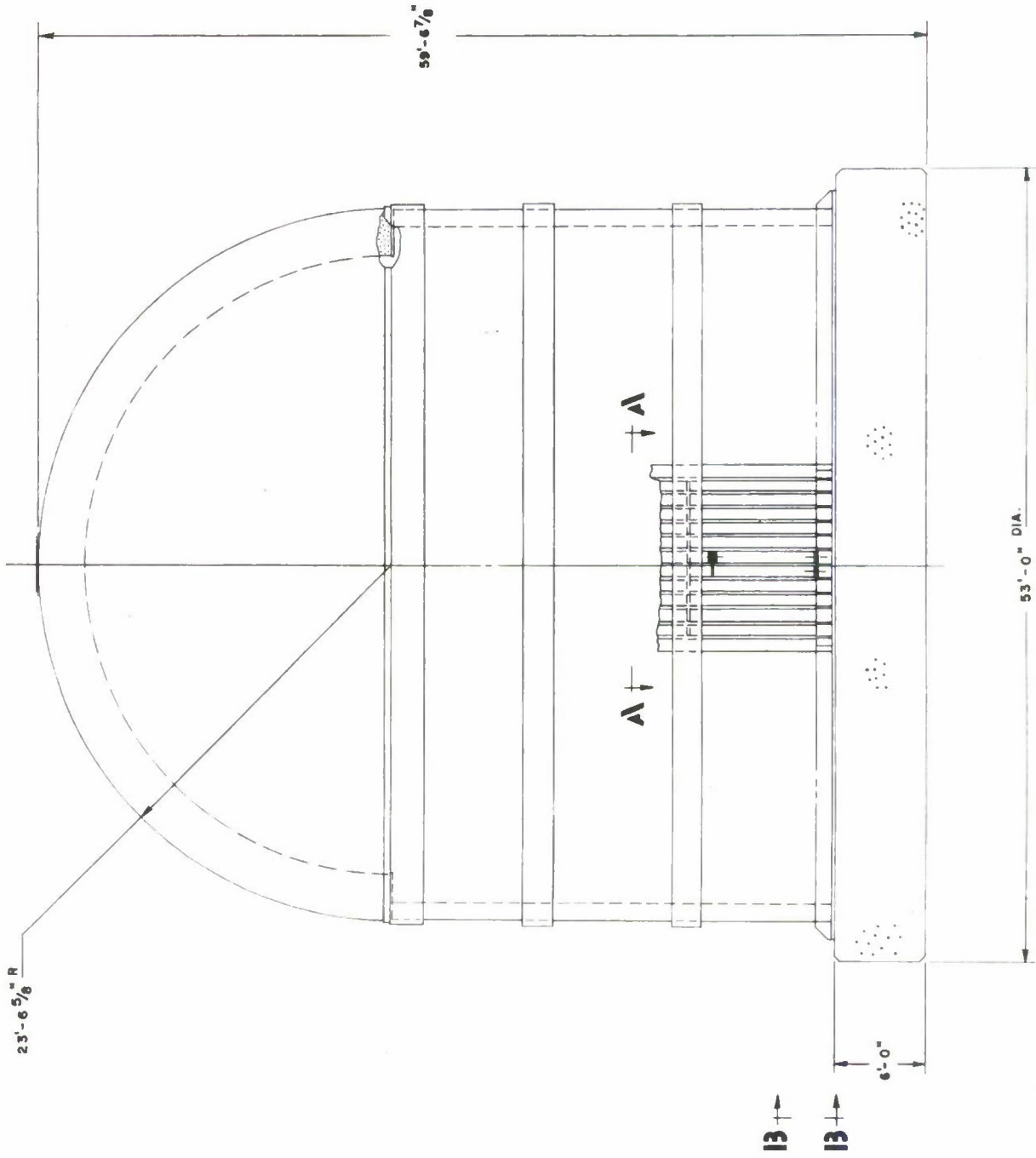
Sodium silicate foam was chosen initially for this application because of its light weight, low cost (relative to other foams) and because it can be foamed in place. The foam is susceptible to deterioration from prolonged moisture exposure, but this limitation would be overcome in the double-dome concept by proper sealing of the domes during fabrication. Another advantage to the use of foam is the attenuation of the impulsive load on the outer dome permitting elastic design of the outer dome without a weight penalty. However, the lack of well-defined fragment stopping capability for the foam caused us to abandon foam in favor of sand.

Fragment stopping capabilities of sand have been well established and are documented in TM 5-1300.<sup>(8)</sup> With an inner dome thickness of 0.5 in., only 3 ft of sand are required to stop the fragment before it contacts the outer dome. These dimensions were established by using the data in TM 5-1300 and the equations for residual mass and velocity given in Reference 9. This approach to defeating the fragment permits the outer dome to remain undamaged prior to sustaining the quasi-static pressure. If fragments were allowed to impact the outer dome, it would be susceptible to the initiation of fast fracture at the sharp edged cracks which are likely to be caused by fragment damage. The outer dome thickness is thus determined by the blast loading only, and the thickness required is 5/8 inch.

With use of sand rather than foam, the inner dome must be larger, but this cost is probably more than offset by the low cost of sand relative to the cost of sodium silicate foam. Also, the additional volume and internal height gained by using sand permits the cylindrical section of the structure to be reduced to 30 ft while still maintaining an internal volume greater than 64,000 cu ft and internal height greater than 40 ft.

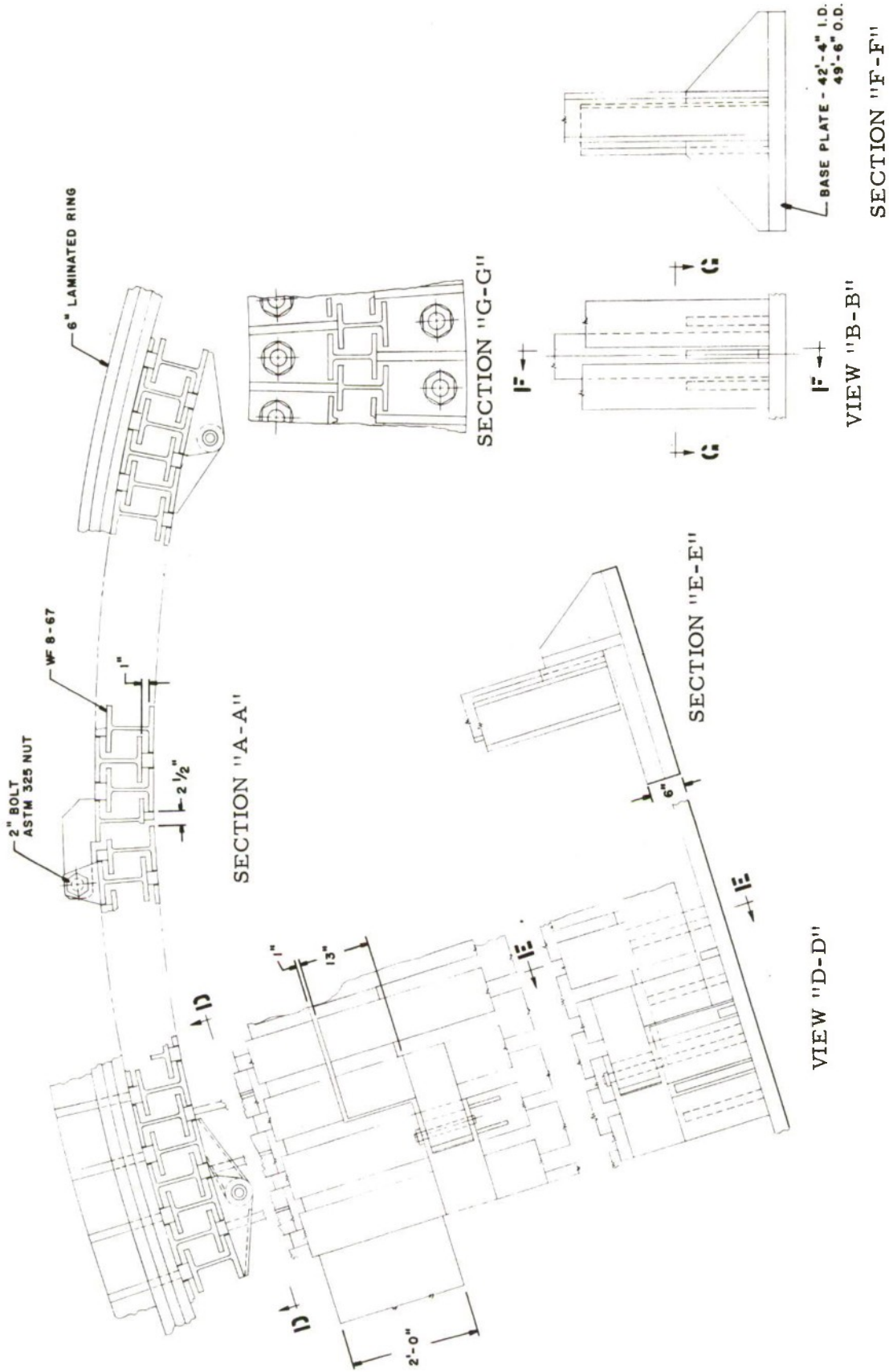
A 30-ft cylindrical I-beam section with the sand-filled double-dome roof is the final configuration suggested by SwRI for the Category 1 prototype shield. This configuration is shown in Figure 15. Details of the cylindrical portion of the structure and its foundation





(a) Overall view

FIGURE 15. FINAL CYLINDRICAL CONCEPT SUGGESTED FOR CATEGORY 1 PROTOTYPE



(b) Door and wall details

FIGURE 15. FINAL CYLINDRICAL CONCEPT SUGGESTED FOR CATEGORY 1 PROTOTYPE (Cont'd)

are similar to those given in Figure 7. Figure 16 gives details of the roof. A weight breakdown for this final configuration as well as for the other concepts considered is included in the next section.

## IV. RESULTS

### A. General Discussion

A number of configurations for a Category I suppressive structure satisfying the guidelines given in Section II were found to be feasible. All of the alternate panel designs can attenuate the external blast overpressures to 50% or better of the free-field values at the intraline distance and closer, and they can also contain the worst-case fragment weighing 1 lb and travelling at 7200 ft/sec. Volume and floor area requirements were easily satisfied by both the rectangular and cylindrical concepts. The only guideline which could not be strictly followed in all concepts was the use of gross plastic deformations short of failure to minimize structural weight and cost. This requirement often conflicted with the fragment defeat requirement, with fragment defeat requiring members which were overstrength for withstanding internal blast loads.

### B. Design Comparisons

We attempted to evaluate the various concepts and configurations studied in terms of both cost and weight. Weight comparisons were made on the basis of steel weight, exclusive of the weight of reinforcing steel in the foundation, internal gridwork and miscellaneous items. Detailed cost estimates could not be obtained, so cost comparisons were based on judgements of relative costs of the different concepts established through discussions with several steel fabricators.\* As discussed in Section B, these judgements of relative cost were often important factors in the decision to discard some of the concepts considered. We attempted to obtain more definitive cost figures for all concepts but were unable to do so. Many steel fabricators were not interested in submitting bids for this structure. Of the three manufacturers who reviewed the drawings and commented on the relative merits of the various configurations, Pittsburgh Des Moines Steel Company and Trinity Industries, Inc., have agreed to perform a cost estimate for the final configuration.† Although a subcontract cost for obtaining these estimates has not been established, indications are that they may be expensive.

The weight breakdown for the various configurations is given in Table II. Because of the many different roof concepts included for the cylindrical structure, weights for the roofs and cylindrical portions are given separately. Weights for the cylindrical concepts were computed for a cylinder which is 40 ft high. As already discussed, this is not the case for the configuration with the dome roof, for which the cylinder is only 30 ft high. This shorter height is reflected in the weights computed for the final cylindrical configuration and included in Table III for comparison with the box configuration.

\*See footnote on page 31.

†No final configuration has been submitted, and no cost estimates have been authorized.

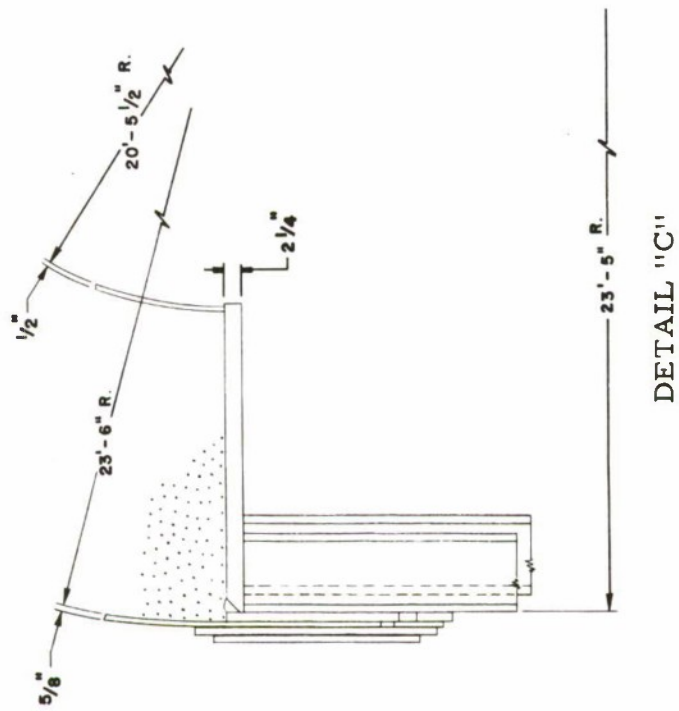
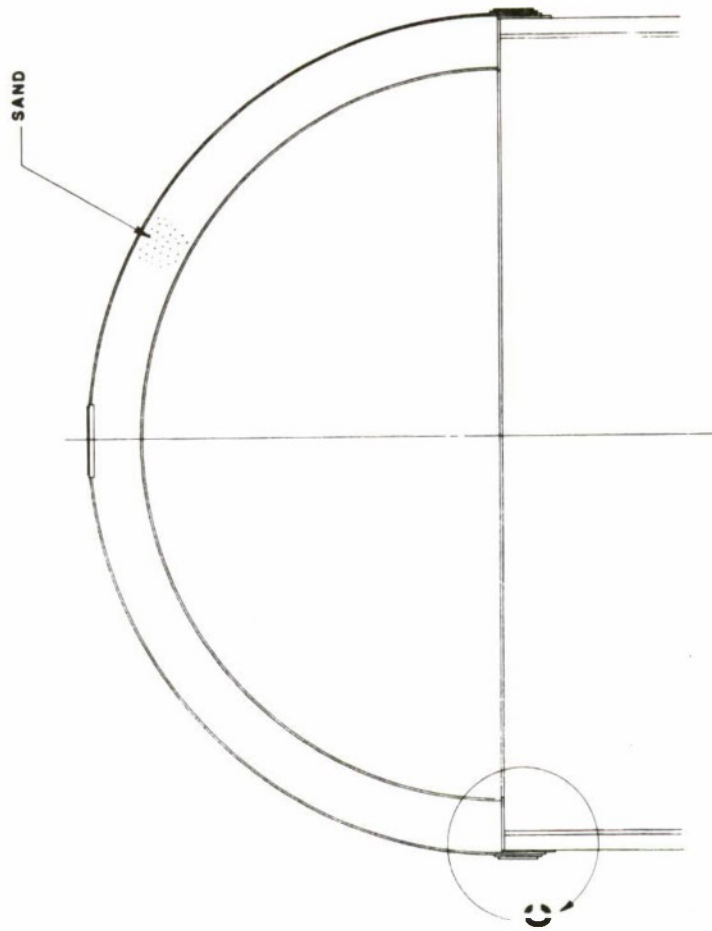


FIGURE 16. SAND FILLED DOUBLE-DOME ROOF

TABLE II. BREAKDOWN OF STEEL WEIGHT (IN TONS)  
FOR PROTOTYPE CATEGORY 1 CONCEPTS

Concepts	Weight of Flat Plate	Weight of Rolled Plate	Weight of Beams	Weight of Angles	Total Weight of Component or Concept
1-Beam Cylinder (40' high)	--	123.9*	420.8	--	666.6
Perforated Cylinder	--	158.4†	--	252.3	410.7
Membrane Roof	115.5	28.8	6.0	--	150.3
Lifting Roof	--	--	--	--	Approx. 300
I Beam Roof	12.1	--	316.2	--	318.3
Double-Dome w/Foam Inner	0.7	72.8	--	--	117.6
Double-Dome w/Sand Outer	19.8‡	44.1	--	--	90.6
Box Concept Frame	236.6	26.7,	925.1	29.5	1721.0
Floor Panels	58.7	44.1	--	50.4	--
420.8	--	--	--	--	--

\*Rings

†Perforated Plate

‡Ring to close bottom of space between the two domes

TABLE III. WEIGHT\* COMPARISON OF CUBE CONCEPT  
WITH FINAL CYLINDRICAL CONCEPT FOR CATEGORY 1  
PROTOTYPE SUPPRESSIVE SHIELD

Concepts	Weight of Flat Plate	Weight of Rolled Plate	Weight of Beams	Weight of Angles	Total Steel Weight Excluding Foundation Reinforcement
Cylindrical I-Beam Cage Domed Roof	19.8	88.5† 70.9‡	315.6		494.8
Box Frame Floor Panels	236.6 58.7 420.8**		925.1	29.5 50.4	1721.0

\*Boundary conditions at foundation. Guided at mid-plane per Figure 23.  
†Lower Ring/Center Ring  
‡Weight of inner and outer domes  
\*\*Plate is perforated

Even though the weight of steel in the reinforced concrete foundation for the cylindrical structure has not been included, the weight savings in using a cylindrical versus a box configuration are apparent. It is also apparent that the I-beam concept is not the lightest cylindrical configuration. The perforated cylinder is. However, based on our conversations with steel fabricators, the I-beam cylinder will be the least expensive to fabricate and erect. The hemispherical roof is the lightest of the roof concepts, primarily because sand has been added for fragment suppression, whereas for the membrane roof, steel only was used. Sand, of course, has not been included in the weights given.

## V. CONCLUSIONS AND RECOMMENDATIONS

The following conclusions were drawn from this study of the Category I shield as applied to a melt pour facility:

- (1) The amount of structural steel in the shield is controlled by the fragment threat rather than by the blast loading.
- (2) Cylindrical geometry produces a lighter and more economical structure than rectangular geometry.
- (3) Where venting is required, interlocking I-beams produce the most economical, although not necessarily the lightest, cylindrical structure.
- (4) Where venting is not required, concentric thin-walled structures, separated by sand, are economical for the particular combination of fragment threat and blast loading specified for this shield.
- (5) A domed roof, consisting of two concentric hemispheres separated by sand, produced the lightest roof in terms of steel weight, for the cylindrical shield.
- (6) Until information is available to show the effect of fragment penetration upon the rupture strength of thin-skinned structural elements such as membranes, domes or cylinders, it is preferable to avoid penetration of these types of load bearing members.
- (7) Reinforced concrete is most suitable for the foundation of the cylindrical shield.

Based on these conclusions we make the following recommendations:

- (1) That a vented shield for the melt pour facility be cylindrical and constructed of inter-locking I-beams, a double-dome roof and a reinforced concrete foundation as shown in Figure 15.

- (2) That fully closed cylindrical and spherical structures of sand-filled double wall construction be investigated for Category I applications.
- (3) That the effect of fragment penetration on the rupture strengths of thin-walled structures under inplane stress be investigated.
- (4) That new ways of founding the structure be investigated. Specifically, a footing-type foundation with a floating inner floor may be both practical and economical. This type of foundation affords greater flexibility in the use of internal space because deep pits in the floor are practical, whereas for slab-type foundations they are not.

## APPENDIX A

### METHODS OF ESTIMATING DYNAMIC AND STATIC LOADING

In Reference 1, the dynamic blast loading on the inner surface of the suppressive structure is separated into two phases, an initial very short duration phase caused by reflection of the first shock wave to reach the walls, followed by a slower rise to a quasi-static pressure which then decays slowly to atmospheric pressure. No additional work has been done which would modify the methods of predicting the properties of the initial reflected wave, but there is an error in the reflected impulses  $I_r$  used in Reference 1 because of an error in curves for  $I_r$  and  $I_s$  in Reference 9. Errors in that reference are noted in Appendix D.

Some additional theoretical and experimental work on quasi-static pressure rises in vented structures, and the blowdown of these pressures, has been reviewed since the earlier study. This review, (Ref. 10), does little to change estimates of the time histories of blowdown pressures, but it does provide an alternate (and hopefully superior) method of presenting scaled parameters associated with this phase of the internal blast loading. We suggest that appropriate nondimensional parameters for venting pressures are:

$$\begin{aligned}
 \bar{P}(\tau) &= \frac{P(t) + p_o}{p_o} & \bar{t} &= \frac{ta_o}{V^{1/3}} \\
 \bar{P}_1 &= \frac{P_{QS} + p_o}{p_o} & \bar{\tau} &= A\bar{t} \\
 \bar{A} &= \frac{\alpha_{\text{eff}}A_S}{V^{2/3}} & \gamma &= \text{gas constant}
 \end{aligned}
 \tag{A-1}$$

Both the theoretical analyses and experimental data in Reference 10 show that the scaled blowdown pressure  $\bar{P}$  is a function of  $\bar{P}_1$ , and  $\bar{\tau}$ . Dependence on  $\gamma$  appears to be quite weak. Plots of scaled blowdown pressure versus scaled time, and scaled venting duration  $\bar{\tau}_{\text{max}}$  versus  $\bar{P}_1$  are given in Reference 10.

An approximate equation for blowdown pressure versus time which seems to agree reasonably well with existing data is given by Kinney and Sewell<sup>(11)</sup>

$$\ln \bar{P} = \ln \bar{P}_1 - 2.130\bar{\tau}
 \tag{A-2}$$

Also, from Kinney and Sewell,<sup>(11)</sup> an approximate expression for  $\bar{\tau}_{\text{max}}$  is

$$\bar{\tau}_{\text{max}} = 0.4695 \ln \bar{P}_1
 \tag{A-3}$$

Integrating Eq. A-3, we obtain an expression for dimensionless impulse in the gas venting phase

$$\bar{I}_g = \frac{1}{2.130} (e^{2.130\bar{\tau}_{\max}} - 1) - \bar{\tau}_{\max} \quad (\text{A-4})$$

where

$$\bar{I}_g = I_g \left( \frac{\alpha_e A_S a_o}{p_o V} \right) \quad (\text{A-5})$$

This equation also seems to agree reasonably well with limited experimental data.

The vent area ratio for this suppressive structure is determined, as in Reference 1, by the requirement that blast overpressure outside the structure be reduced to half or less of the values in absence of the structure, at the intraline or closer. The methods used to establish the  $\alpha_{\text{eff}}$  are the *same* as in Reference 1, except that some definitions of  $\alpha_{\text{eff}}$  have been modified and more data are available to fit the scaled blast overpressures escaping from suppressive structures. The later work is described in some detail in Reference 12. Figure A-1 and Eqs. (A-6) and (A-7) are taken from that reference and are used to determine the  $\alpha_{\text{eff}}$  for this structure. The two equations are:

$$P_s = 677.5 \frac{L^{0.485} \alpha_e^{0.537}}{Z^{1.84}} \quad (\text{A-6})$$

for blast waves emanating from the structure and

$$0.55 \leq L \leq 3.09$$

$$0.025 \leq \alpha_e \leq 0.60$$

$$4.29 \text{ ft/lb}_m^{1/3} < Z < 15.5 \text{ ft/lb}_m^{1/3}, \quad (\text{A-7})$$

and

$$P_s = 962.3/z^{2.057} \text{ for free-field}$$

and

$$4.29 \text{ ft/lb}_m^{1/3} \leq z \leq 15.9 \text{ ft/lb}_m^{1/3}$$

Predicted loading characteristics are summarized in Table A-1.

TABLE A-1. LOADING ON FULL-SCALE CATEGORY 1  
SUPPRESSIVE STRUCTURE

Initial Shock	Quasi-Static Load	Effective Vent Area Ratio
$I_r = 2.43$ psi-sec $P_r = 4053$ psi	$P_{QS} = 165$ psi $t_{max} = 116$ msec	$\alpha_{eff} = 0.0518$

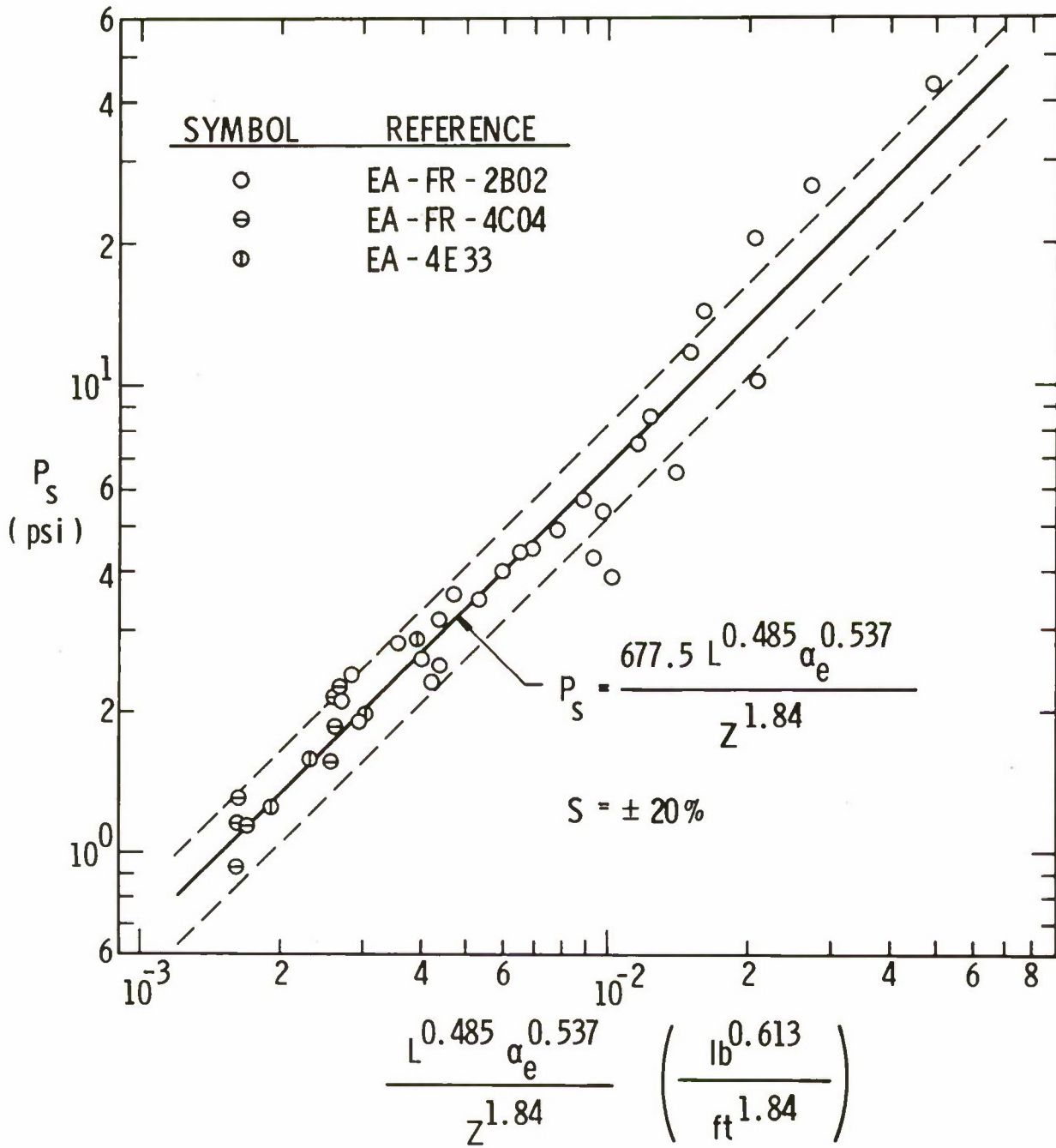


FIGURE A-1. CURVE FIT TO BLAST PRESSURES OUTSIDE NSTL STRUCTURES

## APPENDIX B

### METHODS OF ESTIMATING STRUCTURAL RESPONSE

Numerous equations for estimating the response of structural components were reported in Reference 1. Since that time some of the formulas have been improved and updated and new formulas have been developed as required. In addition, other methods have been used to determine the response of suppressive shields to the internal blast loading. These have included the use of some computer programs developed at SwRI. Both the updated formulas based on the energy methods as well as the response calculations using computer programs will be described in this appendix.

#### A. Energy Methods

Energy solutions, which have been developed by SwRI both in the earlier suppressive structures work reported by Baker, et al<sup>(1)</sup> and more recently by Westine and Cox<sup>(13)</sup>, are summarized in Table B-1. Details of the formula development will not be repeated here. We only emphasize that the formulas were derived for an assumed deformation shape and rigid-plastic material behavior. They relate the final deformed state of the structural element to the element geometry, material properties and blast loading. Definitions of terms in these equations are included in Table B-2.

The formulas of Table B-1 have been placed in a different form than is given in References 1 and 13. Original derivations gave the asymptotes of the response of the structure in the impulsive and in the quasi-static loading realms. In Table B-1 these formulas have been combined to give element response for a combined impulse and quasi-static pressure. This loading is representative of the loads on suppressive structures produced by internal explosions because the impulse produced by the blast wave is followed by a pressure build-up of much longer duration. The formulas reduce to the proper impulsive and quasi-static asymptotes for the case in which either  $p$  or  $i_r$  is zero, respectively.

The combined formulas are based on simultaneous application of an initial impulse and a constant quasi-static pressure. This simultaneous application of the load is supported by preliminary results from the 1/16-scale venting tests<sup>(7)</sup>, which do not show a well defined delay in the build-up of the quasi-static pressure. In fact, the results indicate that a good approximation is to assume an instantaneous rise time for the quasi-static pressure as well as for the initial blast wave.

The error incurred in assuming simultaneous application can be investigated by reference to Figure B-1. The shaded area defined by the intersection of the pressure pulse from the initial blast wave and the quasi-static pressure represents the error incurred by assuming simultaneity of the loading. This impulse relative to the total is indeed very small. Furthermore, the equations are based on a constant quasi-static pressure, that is the decay of the

TABLE B-1. SUMMARY OF ENERGY SOLUTIONS FOR ESTIMATING PLASTIC DEFORMATION OF BLAST-LOADED ELEMENTS

Structural Element	Deformed Shape	Response Formula for Combined Initial Impulse and Quasi-Static Pressure
Cantilever beam	$w = w_0 \left( 1 - \cos \frac{\pi x}{2L} \right)$	$\frac{5.32i_r^2 b^2 L}{\pi \rho A M_p (w_0/L)} = 2.16 \frac{pbL^2}{M_p}$
Simply supported beam, bending only	$w = w_0 \left( 1 - \frac{4x^2}{L^2} \right)$	$\frac{3i_r^2 b^2 L}{4\rho A M_p (w_0/L)} = 12 \frac{pbL^2}{M_p}$
	$w = w_0 \cos \frac{\pi x}{L}$	$\frac{\pi i_r^2 b^2 L}{4\rho A M_p (w_0/L)} = \pi^2 \frac{pbL^2}{M_p}$
Clamped beam, bending only	$w = 2w_0 \left( 1 - \frac{4x^2}{L^2} \right)$	$\frac{i_r^2 b^2 L}{\rho A M_p (w_0/L)} = 32 \frac{pbL^2}{M_p}$
	$w = \frac{16w_0}{L^4} \left( x^2 - \frac{L^2}{4} \right)^2$	$\frac{15i_r^2 b^2 L}{16\rho A M_p (w_0/L)} = 23.09 \frac{pbL^2}{M_p}$
Beam: bending, membrane and strain hardening $N = 1$ , simply supported $N = 2$ , clamped	$w = Nw_0 \left( 1 - \frac{4x^2}{L^2} \right)$	$\frac{i_r^2 b^2}{P_y \rho A} + \frac{4N^{.415} pbL (w_0/L)}{3P_y} = \frac{16NM_y (w_0/L)}{P_y L}$
		$+ \frac{16}{3} \left( \frac{w_0}{L} \right)^2 + \frac{64E_r A (w_0/L)^4}{5P_y}$
Clamped Rectangular plate, bending, membrane and shear	$w = w_0 \cos \frac{\pi X}{2X} \cos \frac{\pi Y}{2Y}$	$\frac{\pi^2 i_r^2 X^2}{8\rho \sigma_y h^4 (w_0/h)} + \frac{pX^2}{\sigma_y h^2} = \frac{\pi^2}{16} \left[ 1 + \left( \frac{X}{Y} \right)^2 \right]$
		$+ \frac{\pi^2}{\sqrt{3}} \left( \frac{h}{Y} \right) \left[ 1 + \frac{X}{Y} \right] + \frac{\pi^4}{128} \left( \frac{w_0}{h} \right) \left[ 1 + \left( \frac{X}{Y} \right)^2 \right]$
		$+ \frac{\pi^2}{4\sqrt{3}} \left( \frac{w_0}{h} \right) \left( \frac{X}{Y} \right)$

TABLE B-1. SUMMARY OF ENERGY SOLUTIONS FOR ESTIMATING PLASTIC DEFORMATION OF BLAST-LOADED ELEMENTS (Cont'd)

Structural Element	Deformed Shape	Response Formula for Combined Initial Impulse and Quasi-Static Pressure
Clamped circular plate, bending and membrane action	$w = w_0 \left(1 - \frac{r}{R}\right)$	$\frac{3i_r^2 R^2}{2\rho\sigma_y h^4 (w_0/h)} + \frac{pR^2}{\sigma_y h^2} = 3 + \frac{3}{2} \left(\frac{w_0}{h}\right)$
Rings supporting I-beams	$\Delta R = \text{constant}$	$\frac{i_r^2 L_B^2}{2A_R^2 \rho \sigma_y \left(1 + \frac{L_B M_B}{\rho A_R C S B R}\right) \left(\frac{\Delta R}{R_i}\right) \left(\frac{R_R}{R_i}\right)} = 1 - \frac{pR L_B}{A_R \sigma_y}$
Hemisphere (dome)	$\Delta R = \text{constant}$	$\frac{i_r^2}{\rho \left(\frac{\Delta R}{R}\right) \sigma} = 1 - \frac{pR}{2\sigma_y h}$
Hemisphere with added mass, $m_a$	$\Delta R = \text{constant}$	$\frac{i_r^2}{\frac{1}{\sigma} \left(\rho + \frac{m_a}{h}\right) \left(\frac{\Delta R}{R}\right)} = 1 - \frac{pR}{2\sigma_y h}$

TABLE B-2. DEFINITION OF SYMBOLS USED IN TABLE B-1

Symbol	Definition
$A$	beam cross-sectional area
$A_R$	ring cross-sectional area
$b$	loaded width of beam
$CSB_R$	circumferential beam spacing in the I-beam cylinder measured at $R_R$
$h$	thickness of plate or dome
$i_r$	specific reflected impulse from initial blast wave, plus reflections if applicable
$L$	length of beam for which the deformation is being determined
$L_B$	length of beam which is restrained by a single ring in the I-beam cylinder
$m_a$	mass per unit area of the inner dome and filler material for the double-dome roof
$m_B$	mass per unit length for the beams in the I-beam cylinder
$M_p$	beam plastic moment
$N$	factor in the beam equation; $N = 1$ for simple support, $N = 2$ for clamped support
$p$	quasi-static pressure
$P_y$	axial yield force of the beam
$r$	radius to arbitrary point on a circular plate
$R$	mean radius of the hemisphere (dome)
$R_R$	mean radius of the ring in the I-beam cylinder
$\Delta R$	radial expansion of the ring or dome
$w$	lateral deflection of a beam or plate at point $x$ or $r$ , respectively
$w_o$	center deflection of a beam or plate
$x$	distance along the beam or plate, normally measured from the center
$X$	short semi-span of the plate
$y$	distance along plate center line normally measured from the plate center
$Y$	long semi-span of the plate
$\rho$	material density
$\sigma_y$	yield strength of the material

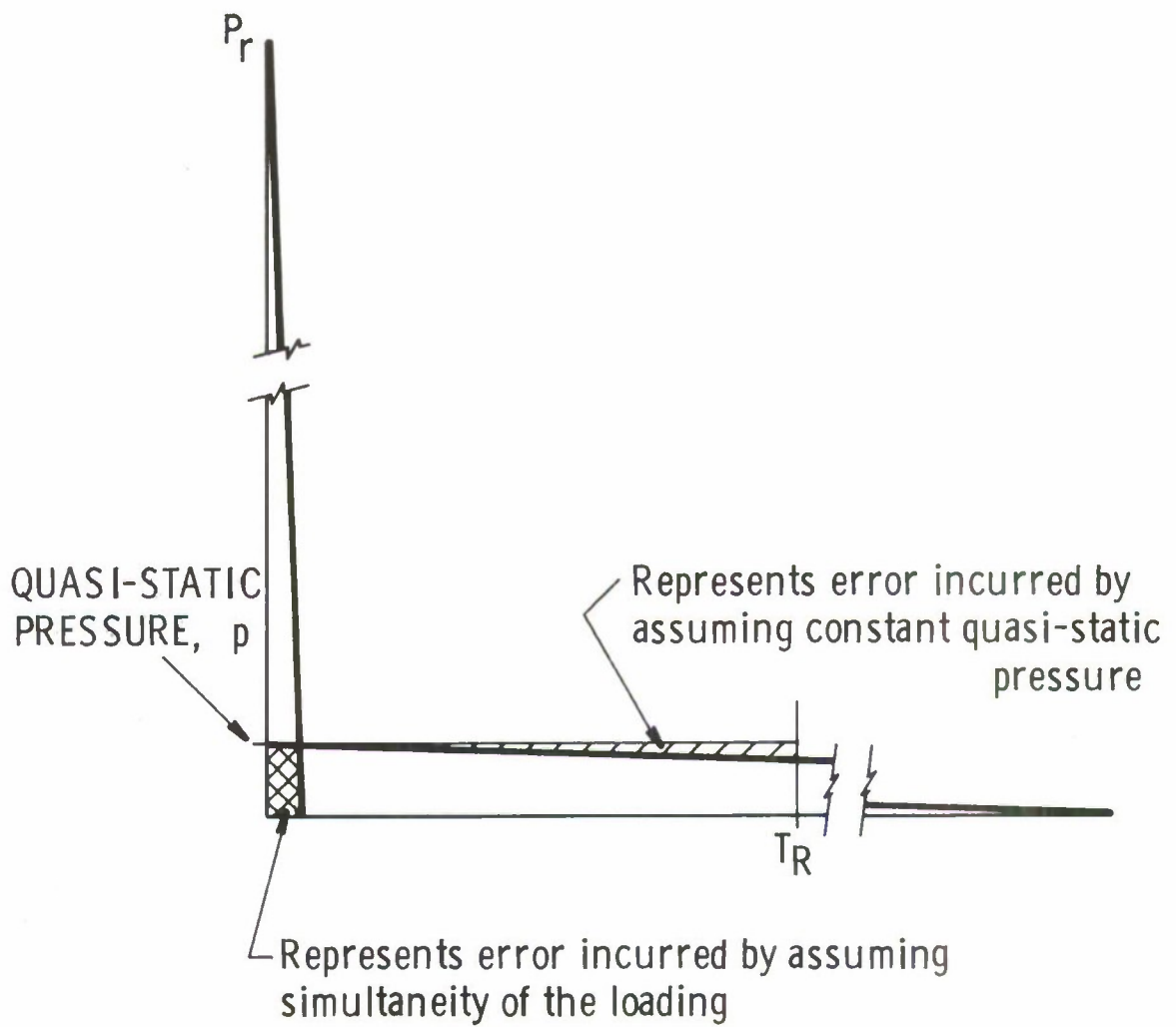


FIGURE B-1. SCHEMATIC OF ERROR INCURRED IN ASSUMING SIMULTANEITY OF LOADING AND CONSTANT QUASI-STATIC PRESSURE

quasi-static pressure over the response time of the structural component,  $T_R$ , has been neglected. This error is indicated by the double cross hatched area shown in the figure. For structures whose response time is short relative to the total duration of the quasi-static pressure, this area is also small.

## B. Application of Computer Programs

Several computer programs have been developed at SwRI for estimating elastic-plastic response of structural elements under dynamic loading. Two of these programs were used to analyze several of the roof concepts for the cylindrical structure and also to study response of the beams and rings in the cylindrical I-beam concept. In some cases these solutions were compared with those obtained from the energy methods, and in other cases the computer programs were used to obtain information not available from the existing energy methods, for example, to investigate coupled response of the beams and rings and to determine beam shearing forces. Brief descriptions of these analyses, including the computer programs used, are included in the following paragraphs.

### 1. I-Beam Cylinder

The computer program DANAX4A was used to study the coupled response of the beams and rings in the I-beam cylindrical concept. This program computes the coupled bending-torsional response of a non-linear beam to arbitrary transient loads. Non-linear springs can be added at selected locations between the beam and ground. A lumped parameter representation of the beam elements is used and a step-by-step integration of the equations of motions of the lumped masses is performed using a linear acceleration predictor-corrector solution procedure.

To compute the response of the I-beams and rings, the conditions shown schematically in Figure B-2 were analyzed. Symmetry has been assumed about a mid-plane through the cylinder. This is strictly true only if the roof and foundation are identical. Even if this is not the case, the response of the beams and ring will be closely approximated by this model, particularly insofar as the reactions at the foundation are concerned.

Some of the results obtained using the computer program for these two cases are summarized in Table B-3. The effect of pinned versus clamped support is demonstrated for both the  $S3 \times 5.7$  beam in the 1/4-scale structure and for the  $W8 \times 67$  beam in the prototype. Also, the effect of ring area on deformation of the ring and upon the shear in the beam at the ring is demonstrated for the Category 1 prototype with the  $W8 \times 67$  beam. Figure B-3 gives the time history of the deflection at the center ring for the prototype with the  $W8 \times 67$  beam for two different ring cross-sectional areas. These results are similar to those used to select a suitable ring area for the Category 1 structure. Application of these results to the selection of beams and rings for the Category 1 prototype structure was discussed in Section III.

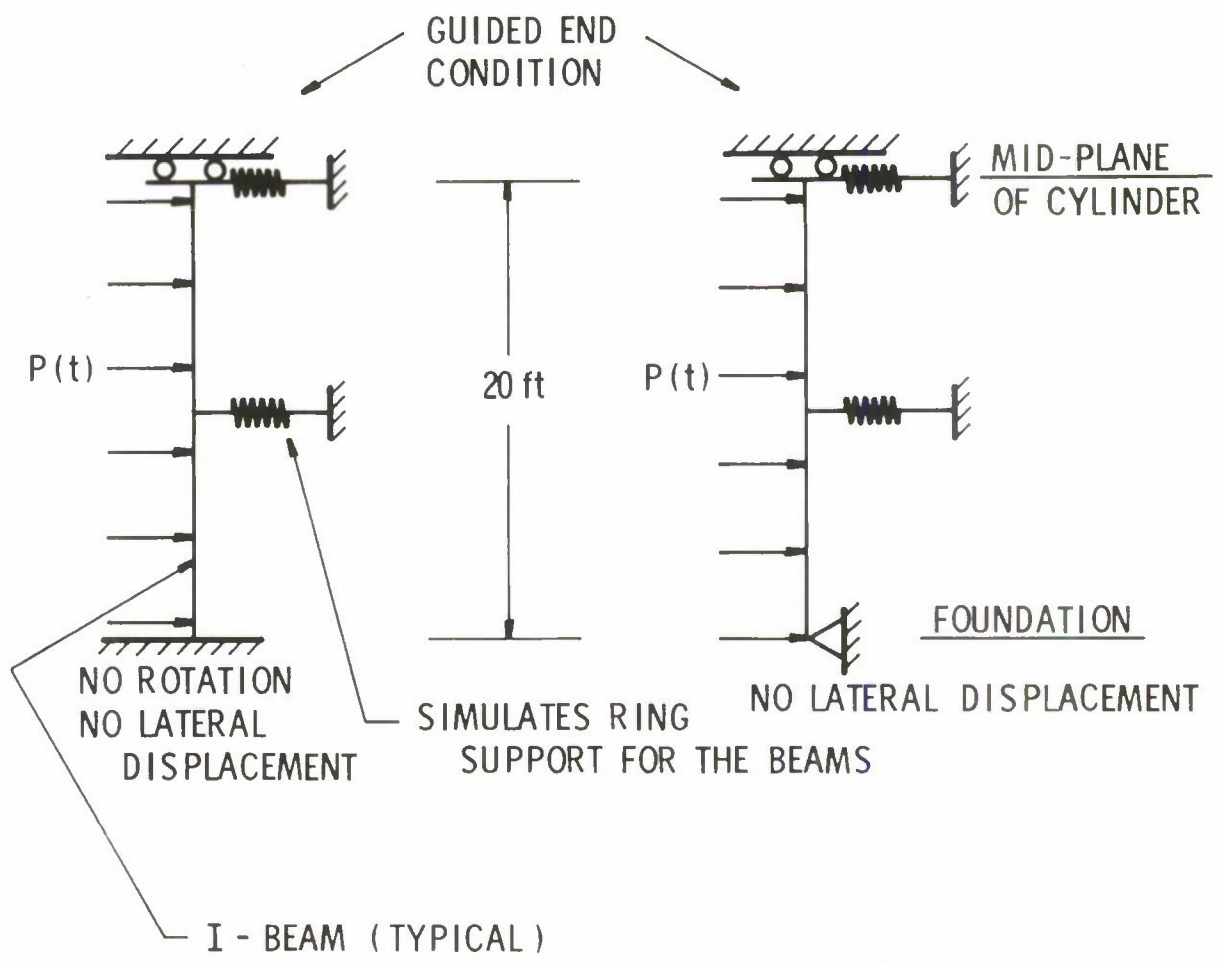


FIGURE B-2. SCHEMATIC OF CASES ANALYZED FOR COUPLED BEAM-RING RESPONSE

TABLE B-3. SUMMARY OF COMPUTER CALCULATIONS  
FOR COUPLED BEAM-RING RESPONSE

Structure	Beam	Conditions	Ring Area (in. <sup>2</sup> )	At Foundation			At Lower Ring		At Center Ring			Maximum Overall Lateral Displacement (in.)
				$\sigma_{s,max}$ (ksi)	$\epsilon_{max}$ (%)	$\Delta R_{max}$ (in.)	$\sigma_{s,max}$ (ksi)	$\epsilon_{max}$ (%)	$\Delta R_{max}$ (in.)	$\sigma_{s,max}$ (ksi)	$\epsilon_{max}$ (%)	
Category 1 Prototype	W10 X 77	Clamped*	217/173†	61.0	8.30	—	47.8	4.20	—	—	—	—
Category 1 Prototype	W10 X 77	Pinned	217/173†	46.4	—	—	47.8	4.76	—	—	—	—
Category 1 Prototype	W8 X 67	Clamped	173	47.1	8.70	—	41.0	3.11	5.58	41.0	3.44	7.75
Category 1 Prototype	W8 X 67	Pinned	173	33.5	—	—	41.0	3.35	7.75	41.0	3.68	7.65
Category 1 Prototype	W8 X 67	Pinned	140	33.5	—	—	38.9	2.62	15.3	38.9	2.80	18.2
Category 1 Model	S3 X 5.7	Clamped	10.8	42.4	6.12	—	32.2	1.27	4.90	30.7	1.77	6.93
Category 1 Model	S3 X 5.7	Pinned	10.8	30.2	—	—	32.2	1.44	6.46	32.2	1.54	8.08
1/16-Scale Box	S3 X 5.7	Clamped	8.75	41.4	0.80	—	—	—	—	—	—	0.11

\*Boundary conditions at foundation guided at mid-plane per Figure 23.

†Lower Ring/Center Ring

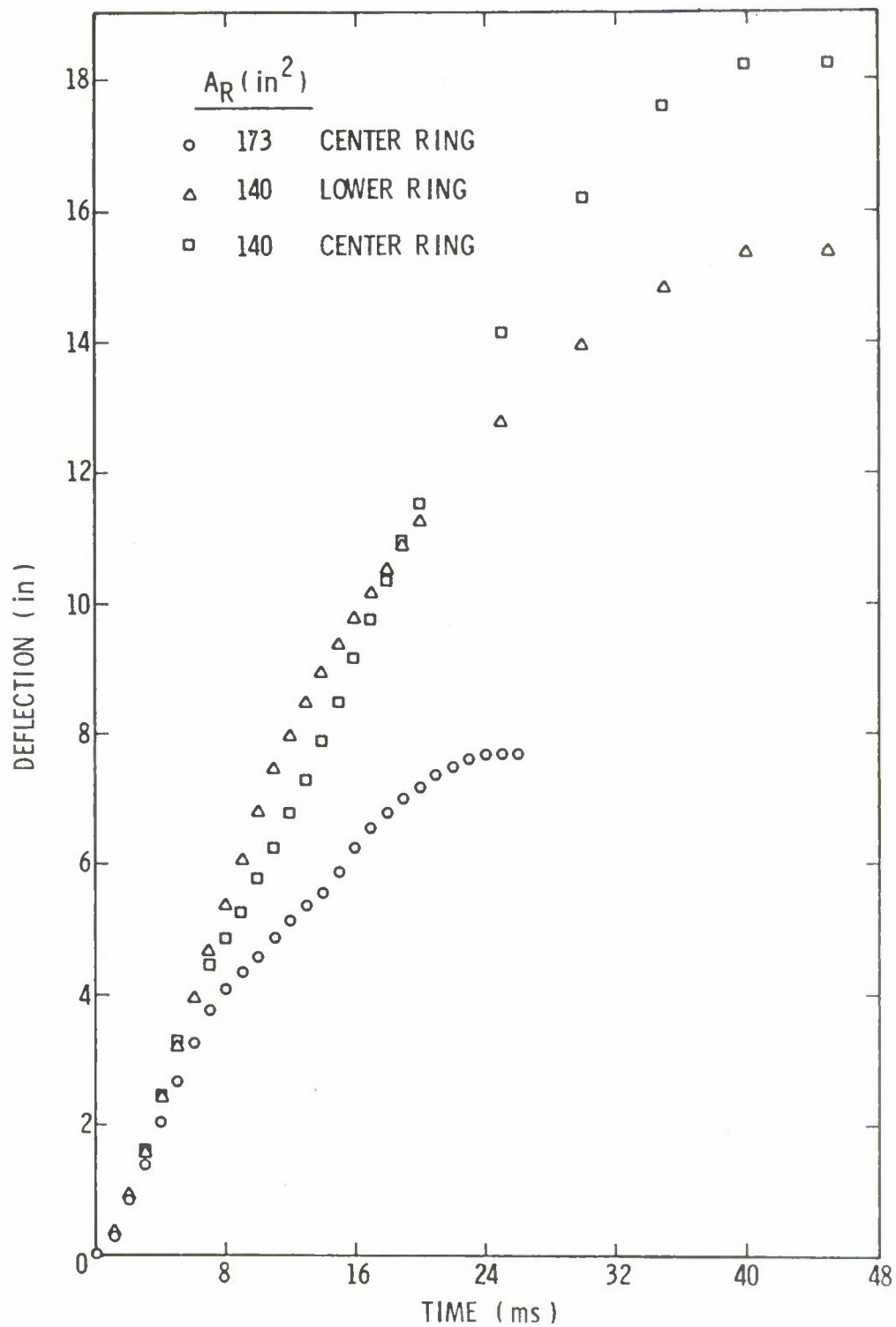


FIGURE B-3. RADIAL DEFLECTION OF CENTER RING-CATEGORY 1 CYLINDRICAL SHIELD WITH W8 x 67 BEAMS

## 2. *I-Beam Roof Concept*

In addition to the analysis of the I-beams and rings in the cylindrical portion of the structure, DANAX4A was used for a single response calculation of the I-beam roof concept. Realizing that only commercially available beams would prove economical for the roof members, we used the program to compute the response of this roof concept (see Section III), constructed with the largest commercially available beams as the spokes. W8 X 67 beams were interlaced between the radial members.

The lumped mass model used to study the response of this concept is shown in Figure B-4. An outline of the portion of the roof included in the model is shown with phantom lines. Weights and loads applied at the mass points were based on the pie-shaped section. In general, they increase linearly with increasing distance from the center. Stiffness properties were based on the W14 X 730 spoke member and thus were constant along the length of the model except in the hub region where the spokes intersect.

Even though the W14 X 730 beam was known to be inadequate for the peak quasi-static pressure, it is difficult to predict how much deformation will occur without resorting to a calculation of the response-time history. This is true because the response time of the roof undergoing plastic deformation is unknown and the quasi-static pressure is, of course, decreasing at a predetermined rate. Nevertheless, the calculation confirmed our suspicions that this roof concept was underdesigned. Results show no apparent deceleration of the roof 125 ms after the detonation when the center deflection had reached 14 ft. At this time the quasi-static pressure had dropped to about 50 psi. As discussed in Section III, this concept was dropped from further consideration.

## 3. *Membrane Roof Concept*

Response of the membrane roof concept was studied using another SwRI program labeled DANAXX5. This program computes the time-history of lateral response of a pin-jointed framework to time-dependent applied forces, taking into account the change in stress in each member produced by its change in length. Thus, this program can be used conveniently to model a membrane subject to timed-varying surface pressures. Initial tension is added to duplicate the contribution of bending to the initial stiffness.

We had planned to use the program to investigate the differences in response of the membrane produced by different boundary constraints, that is, full in-plane constraint versus constraint more nearly approximating that afforded by the I-beam and perforated cylinders. Other factors, discussed in Section III, caused us to abandon the membrane concept before the study was completed. However, using the model of Figure B-5 the response of a fully restrained roof was determined. Results showed a peak center deflection of 85 in. and a peak strain in the members of 13.4%. The deflection time-history and the strain time-history at typical points within the membrane are shown in Figures B-6 and B-7. These deflections and strains are keyed to nodal points and members in Figure B-7. It is apparent from Figure

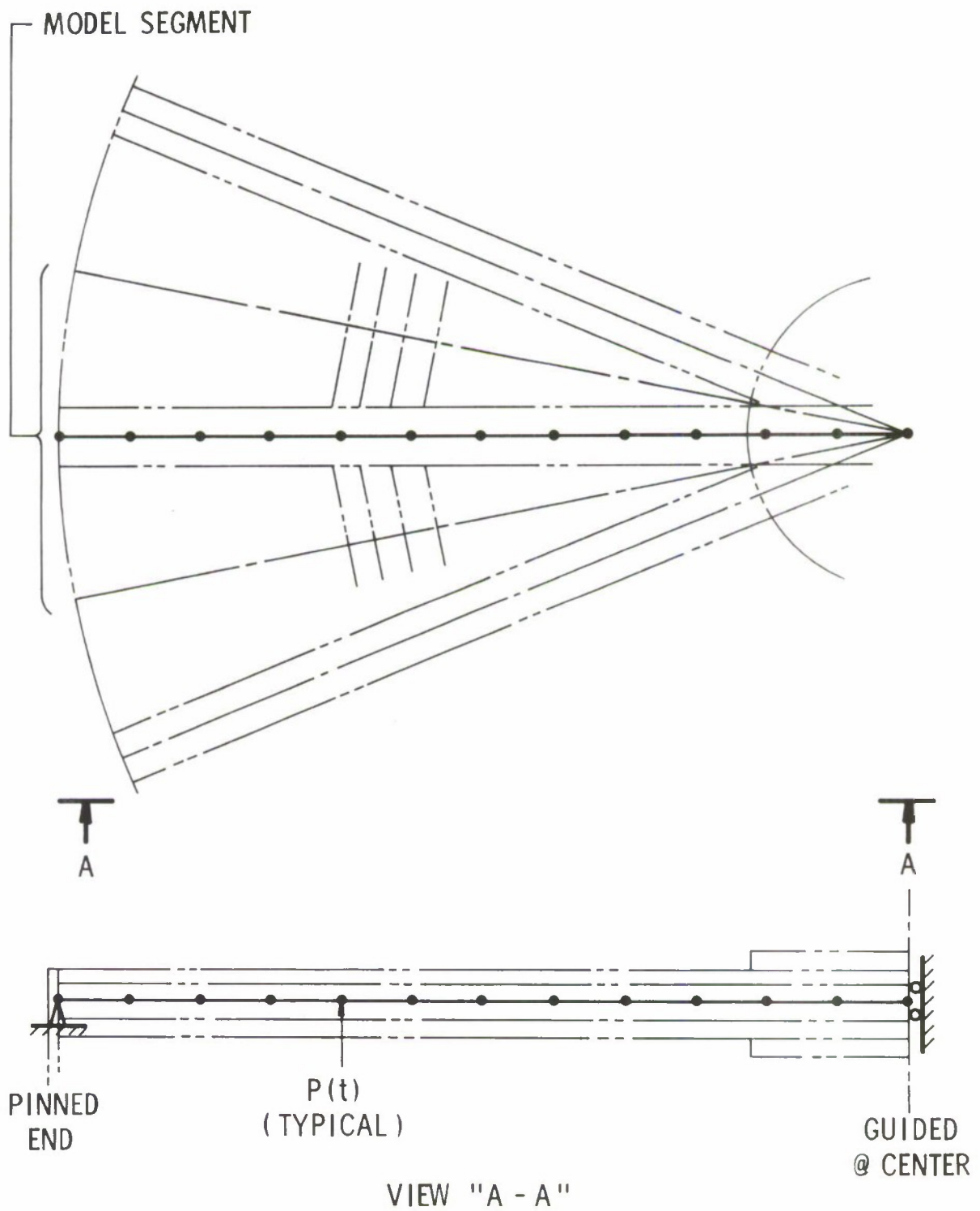


FIGURE B-4. LUMPED-PARAMETER MODEL OF SEGMENT FROM THE I-BEAM ROOF CONCEPT

1, 2 - TYPICAL NODE NUMBERS

⑤⑧, ⑨⑩ - TYPICAL MEMBER NUMBERS

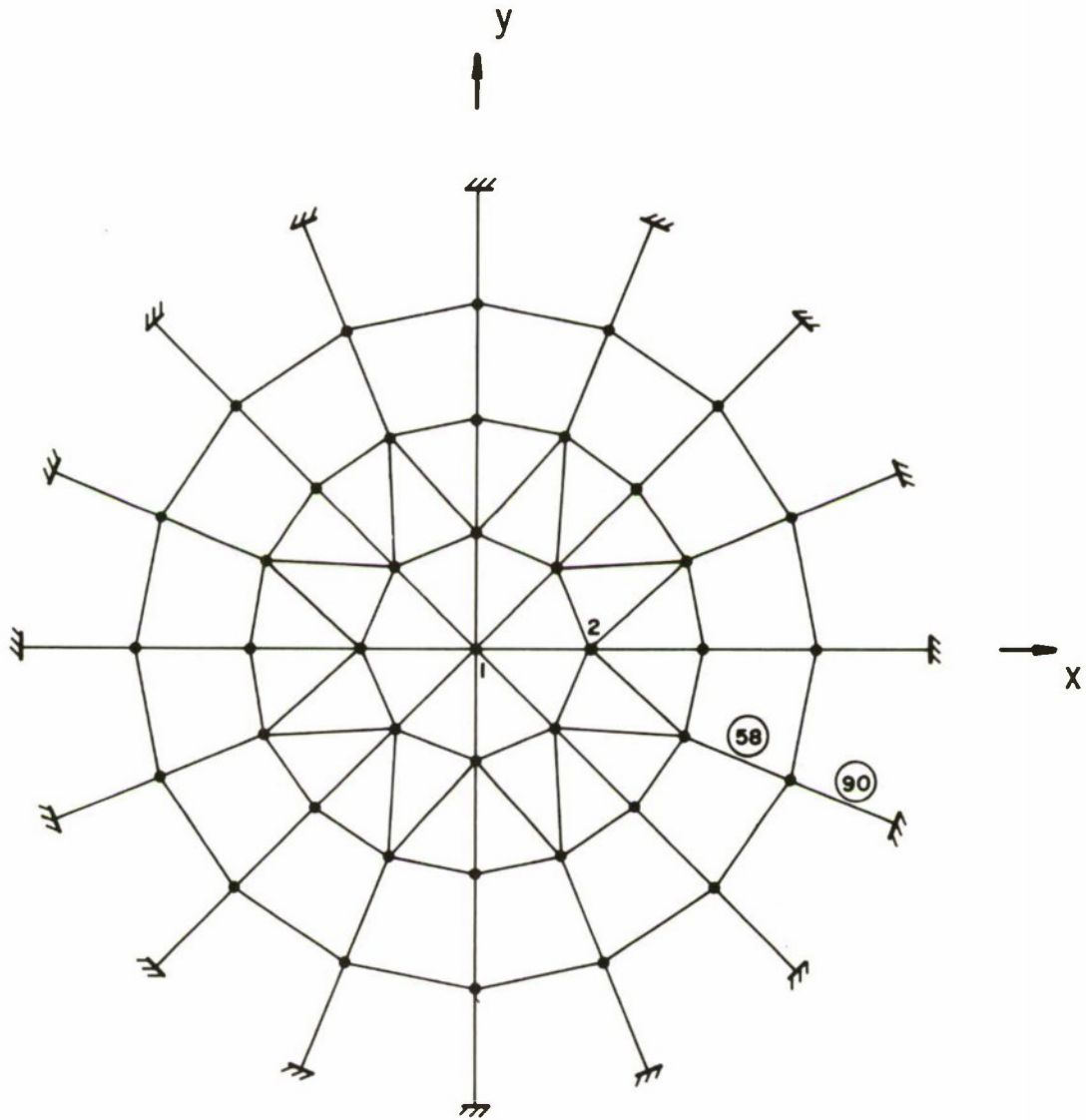


FIGURE B-5. MODEL OF THE MEMBRANE ROOF

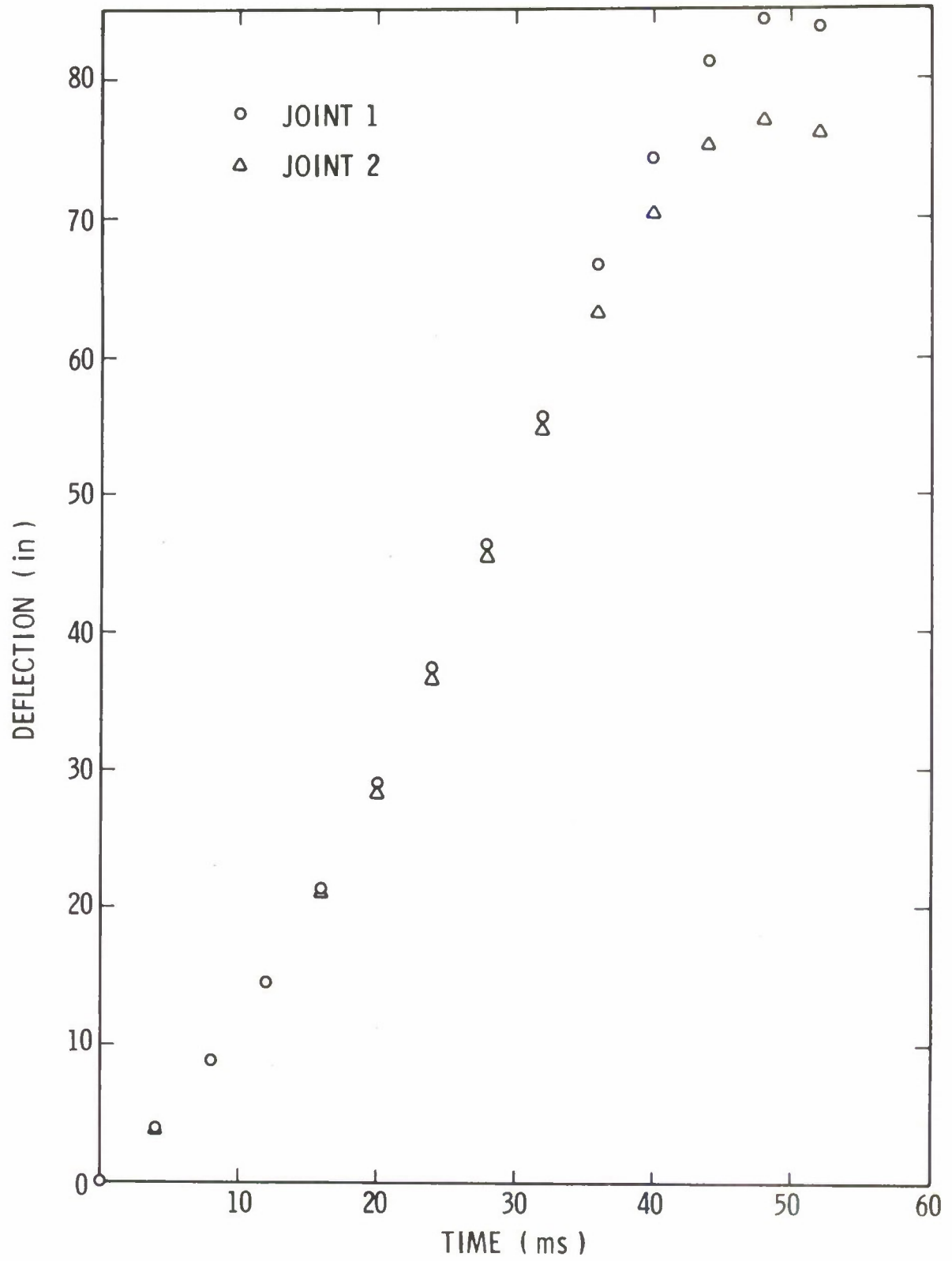


FIGURE B-6. VERTICAL DEFLECTIONS OF THE MEMBRANE ROOF CONCEPT

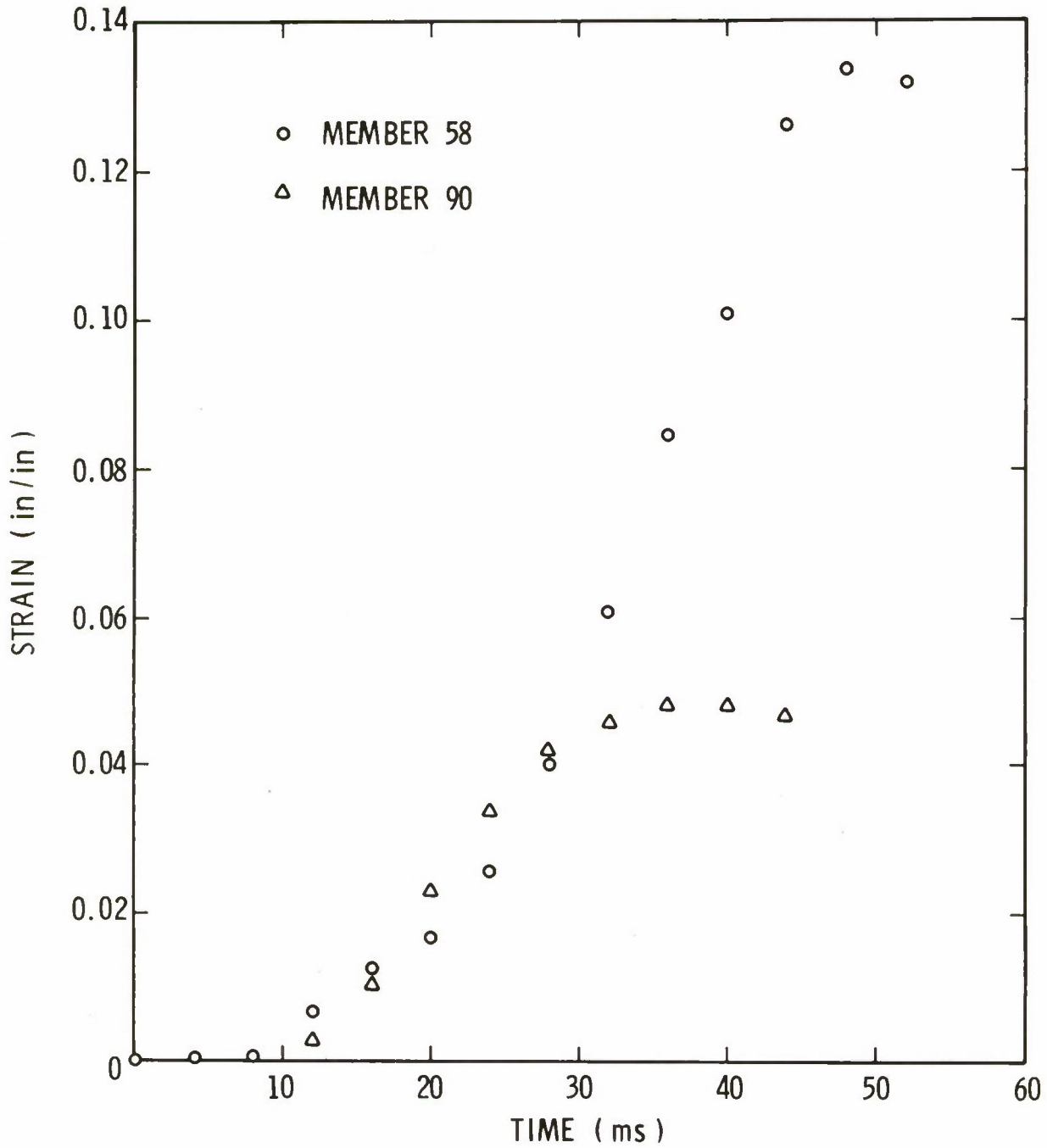


FIGURE B-7. MEMBER AXIAL STRAINS IN THE MEMBRANE ROOF CONCEPT

B-7 that uniform strain, characteristic of a true membrane, was not achieved with the model used.

Peak deflections and strains computed from the program were compared with the energy solutions which gave a peak center deflection of 87.28 in. and a maximum strain of 4.8%. While the peak deflections agree very well, the peak strain predicted by the program far exceeds that predicted by the energy solution. The discrepancy here is due to non-uniformity in the lumped parameter model used in the computer program. The energy solution was based on a uniform strain assumption<sup>(13)</sup>.

## APPENDIX C

### METHODS FOR ESTIMATING FRAGMENT PENETRATION

One of the requirements for the Category 1 suppressive shield is to contain all primary fragments. An estimate was made in Reference 2 to determine the size and velocity of the worst-case primary fragment from a survey of fragments resulting from explosions of large bombs. The size of the bombs analyzed approaches the order of magnitude of explosive in the melt kettle and the charge weight to container weight ratio,  $W/W_e$ , was approximately one. This study concluded that the largest fragments resulting from the explosion of a 2500-lb melt kettle would be no larger than 1 lb<sub>m</sub> and that its velocity was 7200 fps. Thus, the Category 1 shield was designed to defeat this fragment threat.

To estimate the thickness of steel in one layer or multiple spaced layers required to stop the worst case primary fragment, Reference 14 provides equations for computing residual velocity and mass of a fragment perforating a target or series of targets. An estimate of the logarithm of the loss of velocity of a fragment perforating a target is given by:

$$\log_{10}(V_S - V_R) = b_0 + \sum_{i=1}^4 b_i \log_{10} X_i \quad (C-1)$$

where

$V_S$  = fragment striking velocity (ft/sec)

$V_R$  = residual velocity of the largest piece of the original fragment after perforation of the target (ft/sec)

$X_1$  = target thickness (in.)

$X_2$  = fragment striking mass (grains) =  $M_S$

$X_3$  = secant of the angle of impact obliquity of the fragment (angle between fragment trajectory and normal to target)

$X_4$  = fragment striking velocity (ft/sec)

and  $b_i$  are parameter estimates for homogeneous mild steel,

$b_0$  = 3.9064 (coefficient estimate)

$b_1$  = 0.9496 (target thickness coefficient estimate)

$b_2$  = -0.3603 (striking mass coefficient estimate)

$$b_3 = 1.2842 \text{ (impact obliquity coefficient estimate)}$$

$$b_4 = 0.1929 \text{ (striking velocity coefficient estimate)}$$

A similar relationship gives the loss of mass of a fragment perforating a target. The equation is:

$$\log_{10}(M_S - M_R) = b_0 + \sum_{i=1}^4 b_i \log_{10} X_i \quad (\text{C-2})$$

where

$$M_S = \text{fragment original mass (grains)}$$

$$M_R = \text{residual mass of the fragment (grains)}$$

$$X_1 = \text{target thickness (in.)}$$

$$X_2 = \text{fragment striking mass (grains)} = M_S$$

$$X_3 = \text{secant of the angle of impact obliquity of the fragment (angle between fragment trajectory and normal to target)}$$

$$X_4 = \text{fragment striking velocity (ft/sec)}$$

and again  $b_i$  are estimates for homogeneous mild steel,

$$b_0 = -2.2776 \text{ (coefficient estimate)}$$

$$b_1 = 0.1885 \text{ (target thickness coefficient estimate)}$$

$$b_2 = 0.9145 \text{ (striking mass coefficient estimate)}$$

$$b_3 = 0.1958 \text{ (impact obliquity coefficient estimate)}$$

$$b_4 = 0.6394 \text{ (striking velocity coefficient estimate)}$$

These two equations are applied to the array of targets as long as there are residual fragment velocity and residual fragment mass. When a target has succeeded in stopping a fragment, a negative residual velocity is obtained; then it is necessary to compute the depth of penetration into that particular target. This is accomplished in the case of a steel fragment, with a normal trajectory, penetrating a mild steel target using the following equation:

$$P = 0.112 M^{1/3} (0.001 V)^{4/3} \quad (\text{C-3})$$

where

$P$  = penetration (in.)

$M$  = fragment mass (oz)

$V$  = fragment striking velocity (ft/sec)

According to Reference 2, this equation was developed from a series of experiments conducted within the following limits.

$.197 < M < .310$  oz.

$1690 < V < 3775$  fps

$.125 < T < .375$  in. (plate thickness)

Using all of these equations, a series of graphs was developed in Reference 2 to show the total thickness of mild steel required to defeat different size fragments at three velocities. The number of plates in a series varies from 1 to 4, and all angles of impact are normal to the target. Figure C-1 shows one of these graphs which corresponds to the primary fragment of interest for the Category 1 shield. The abscissa,  $W/W_c$ , is the ratio of the explosive weight to the casing weight.

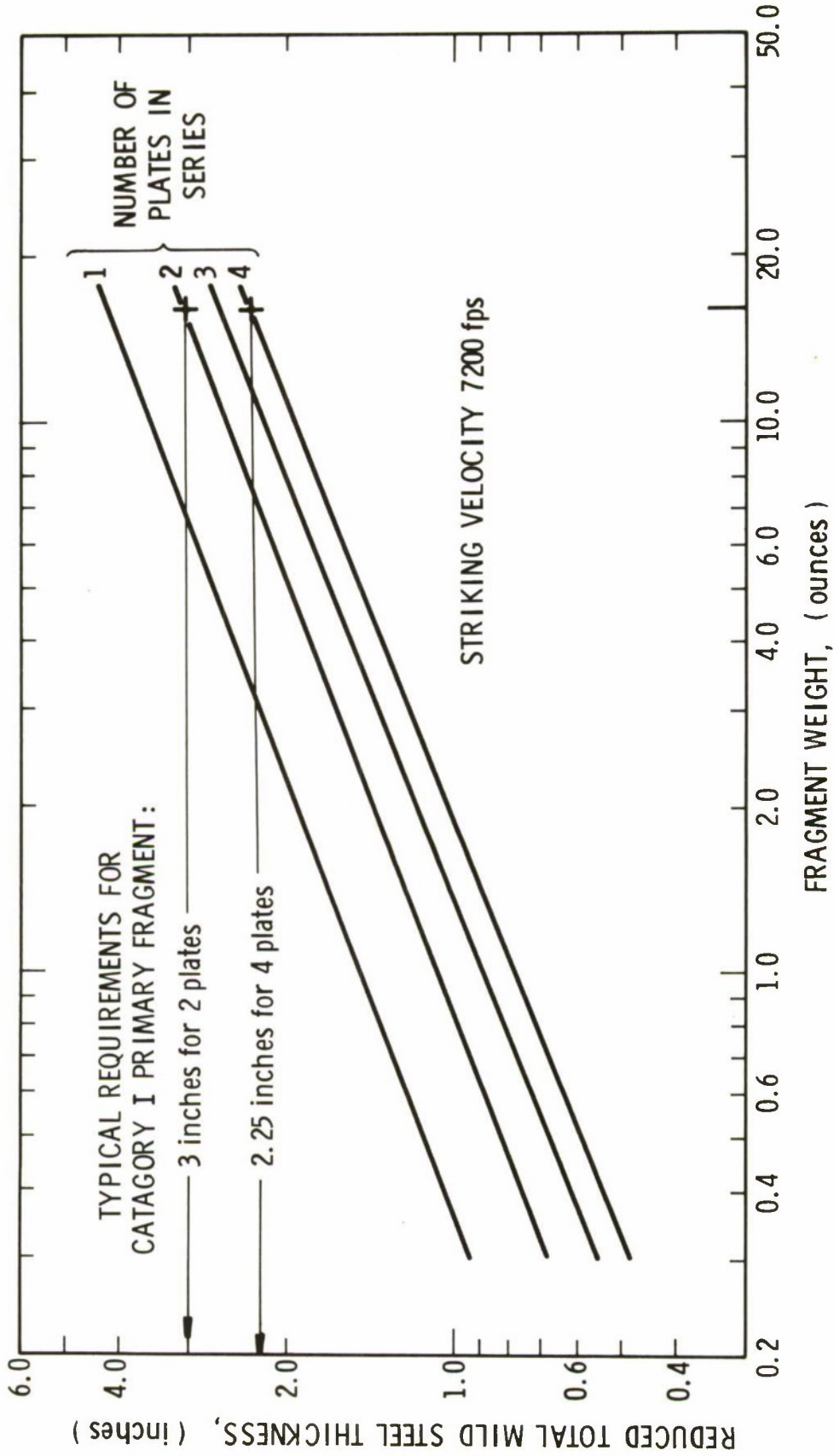


FIGURE C-1. FRAGMENT CONTAINMENT FOR  $w/w_c = 1$

APPENDIX D. ERRATA IN CHAPTER 6,  
*Explosions in Air*, W.E. Baker,  
 U. of Texas Press, 1973

Compiled data for two integrated blast wave parameters, and other quantities derived from these two parameters, are in error. All but one of the incorrect parameters can be corrected by multiplication by a constant for all scaled distances  $\bar{R}$ .

The basic parameters in error are scaled side-on impulse  $\bar{I}_s$  and scaled reflected impulse  $\bar{I}_r$ . Values for  $\bar{I}_s$  and  $\bar{I}_r$  which are listed in Table 6.5, p. 160, and plotted on Figure 6.3 on p. 161 and in the large foldout, should be multiplied by the correction factor 1.630. The parameter  $\bar{I}_s$  reappears in Table 6.6, and should also be multiplied by 1.630. The columns for  $(\bar{I}_s/\bar{P}_s\bar{T}_s)$  and  $b$  in Table 6.6 should also be corrected by multiplication by 1.630, as should values read from the graph 6.3 for  $b$ .

The parameter  $(d\bar{p}/d\bar{t})|_o$  in Table 6.6 cannot be corrected by simple multiplication. Corrected values are given in the following table.

$\bar{R}$	$(d\bar{p}/d\bar{t}) _o$
0.100	-9.34 + 4
0.150	-2.78 + 4
0.200	-6.24 + 3
0.250	-2.18 + 3
0.300	-9.38 + 2
0.400	-2.63 + 2
0.500	-1.07 + 2
0.600	-5.57 + 1
0.800	-2.22 + 1
1.00	-1.137 + 1
2.00	-2.03
4.00	-5.47 - 1
6.00	-3.02 - 1
8.00	-1.95 - 1
10.0	-1.42 - 1
20.0	-5.93 - 2
40.0	-2.58 - 2
60.0	-1.64 - 2
100.0	-9.25 - 3
500.0	-1.43 - 3
1000.0	-6.44 - 4

Finally, the constant in Eq. (6-26), p. 159, must be corrected. That equation should read

$$\bar{I}_s = \frac{4.69 \times 10^{-2}}{\bar{R}} \quad (6-26)$$

## REFERENCES

1. W.E. Baker, P.S. Westine, P.A. Cox and E.D. Esparza, "Analysis and Preliminary Design of a Suppressive Structure for a Melt Loading Operation," Tech. Rep. No. 1, Contract DAAD05-74-C-0751, Southwest Research Institute, San Antonio, Texas, March 4, 1974.
2. J. Coutinho, N. Hagsis and J. Liu, "Current State of Design Procedures for Suppressive Structures," RAMD Interim Note No. R-29, U.S. Army Systems Analysis Agency, Aberdeen Proving Ground, Md., May 1974.
3. W.E. Baker, Letter dated June 27, 1974, to J. Coutinho, U.S. Army Materiel Systems Analysis Agency, Aberdeen Proving Ground, Md., 21005.
4. J.R. Johnson and R.E. Mioduski, "Estimation of Loss of Velocity and Mass of Fragments During Target Perforation," BRL Memorandum Report No. 1777, Aberdeen Proving Ground, Md., Sept. 1966.
5. P.A. Cox and E.D. Esparza, "Preliminary Design of a Suppressive Structure for a Melt Loading Operation," Edgewood Arsenal Contractor Report EM-CR-76028, Report No. 7, Contract DAAA15-75-C-0083, SwRI, San Antonio, Texas, 1975.
6. D.M. Koger, Letter dated 12 Nov. 1974 to J.L. McKivrigan, SAREA-MT-H, with enclosure.
7. R.N. Schumacher and W.O. Ewing, Jr., "Blast Attenuation Outside Cubical Enclosures Made Up of Selected Suppressive Structure Panel Configurations," BRL Interim Memorandum Report No. 376, April 1975.
8. "Structures to Resist the Effects of Accidental Explosions," Department of the Army Technical Manual TM 5-1300, June 1969.
9. W.E. Baker, *Explosions in Air*, University of Texas Press, Austin, Texas 1973.
10. W.E. Baker and G.A. Oldham, "Estimates of Blowdown of Quasi-static Pressures in Vented Chambers," Edgewood Arsenal Contractor Report EM-CR-76029, Rep. No. 2, Contract DAAA15-75-C-0083, SwRI, San Antonio, Texas, 1975.
11. G.F. Kinney and R.G.S. Sewell, "Venting of Explosions," NWC Technical Memorandum 2448, Naval Weapons Center, China Lake, California, July 1974.
12. E.D. Esparza, "Estimating External Blast Loads from Suppressive Structures," Edgewood Arsenal Contractor Report EM-CR-76030, Rep. No. 3, Contract DAAA15-75-C-0083, SwRI, San Antonio, Texas, 1975.
13. P.S. Westine and P.A. Cox, "Additional Energy Solutions for Predicting Structural Deformations," Edgewood Arsenal Contractor Report EM-CR-76031, Rep. No. 4, Contract DAAA15-75-C-0083, SwRI, San Antonio, Texas, 1975.

14. B. Bertrand, C. Brown, D.J. Dunn, et al., "Suppressive Structures—A Quick Look," BRL Interim Memorandum Report No. 190, Aberdeen Proving Ground, Maryland, Feb. 1974.

## DISTRIBUTION OF SUPPRESSIVE SHIELDING REPORTS

Addressee	No. of Copies
Commander Rocket Propulsion Laboratory Attn: Mr. M. Raleigh Edwards Air Force Base, CA 93523	1
Commander HQ, Armament Development Test Center Attn: DOM/Mr. S. Reither Eglin Air Force Base, FL 32542	1
Commander Hill Air Force Base Attn: MMNTR/Mr. Cummings Clearfield, UT 84406	1
Commander Norton Air Force Base Attn: AFISC-SEV/Mr. K. Collinsworth San Bernardino, CA 92409	1
Commander Air Force Civil Engineering Center Attn: AFCEC-DE/LTC Walkup Tyndall Air Force Base Panama City, FL 32401	1
Commander HQ Air Force Logistics Command Attn: MMWM/CPT D. Rideout IGYE/Mr. K. Shopher Wright-Patterson Air Force Base Dayton, OH 45433	1 ea
Commander Naval Ordnance Systems Command Attn: Code ORD 43B/Mr. A. Fernandes Washington, DC 20360	1
Commander Explosives Safety Attn: ADTC/SEV (Mr. Ron Allen) Eglin Air Force Base, FL 32542	1

Commander Bureau of Naval Weapons Attn: Code F121/Mr. H. Roylance Department of the Navy Washington, DC 20360	1
Commander Naval Ship Research & Development Center Attn: Code 1747/Mr. A. Wilner Bethesda, MD 20034	1
Commander Naval Explosive Ordnance Disposal Facility Attn: Code 501/Mr. L. Wolfson Indianhead, MD 20640	1
Commander Naval Ordnance Systems Command NAPEC Naval Ammunition Depot Attn: ORD-04M/B/X-5/Mr. L. Leonard Crane, IN 47522	1
Commander US Naval Surface Weapons Center Attn: Mr. J. Proctor Whiteoak, MD 20904	1
Chairman DOD Explosives Safety Board Attn: COL P. Kelly, Jr. Forrestal Building GB-270 Washington, DC 20314	5
Joint Army-Navy-Air Force Conventional Ammunition Production Coordinating Group USA Armament Command Attn: Mr. Edward Jordan Rock Island, IL 61201	5
HQDA (DAEN-MCC-I/Mr. L. Foley) Washington, DC 20314	1
HQDA (DAEN-MCE-D/Mr. R. Wight) Washington, DC 20314	1
Director USAMC Field Safety Activity Attn: AMXOS-TA/Mr. Olson Charlestown, IN 47111	1

Commander 1 ea  
US Army Materiel Command  
Attn: AMCCG  
AMCRD/Dr. Kaufman  
AMCSF/Mr. W. Queen  
AMCPM-CS/COL Morris  
5001 Eisenhower Ave.  
Alexandria, VA 22333

Office of the Project Manager for 3  
Munition Production Base Modernization  
and Expansion  
Attn: AMCPM-PBM-E/Mr. Dybacki  
USA Materiel Command  
Dover, NJ 07801

Commander 1 ea  
US Army Armament Command  
Attn: AMSAR-EN/Mr. Ambrosini  
AMSAR-SC/Dr. C. Hudson  
AMSAR-SF/Mr. J. Varcho  
AMSAR-TM/Mr. Serlin, Mr. T. Fetter, Mr. S. Porter  
AMSAR-MT/Mr. A. Madsen, Mr. G. Cowan, CPT Burnsteel  
Rock Island Arsenal  
Rock Island, IL 61201

Commander 1 ea  
USAMC Ammunition Center  
Attn: Mr. J. Byrd  
AMXAC-DEM/Mr. Huddleston  
Mr. Sumpterer  
Savanna, IL 61074

Commander 1 ea  
Frankford Arsenal  
Attn: Mr. F. Fidel, Mr. E. Rempier  
Bridge and Tacony Sts.  
Philadelphia, PA 19137

Commander  
Picatinny Arsenal  
Attn: Mr. Saffian 3  
Mr. J. Cannovan 1 ea  
Mr. Hickerson  
Mr. I. Forsten  
Dover, NJ 07801

Commander USA Test and Evaluation Command Attn: AMSTE-NB Aberdeen Proving Ground, MD 21005	1
Commander Dugway Proving Ground Attn: Dr. Rothenburg Mr. P. Miller Dugway, UT 84022	1 ea
Commander Cornhusker Army Ammunition Plant Grand Island, NE 68801	1
Commander Indiana Army Ammunition Plant Charleston, IN 47111	1
Commander Iowa Army Ammunition Plant Burlington, IA 52502	1
Commander Joliet Army Ammunition Plant Joliet, IL 60436	1
Commander Kansas Army Ammunition Plant Parsons, KS 67357	1
Commander Longhorn Army Ammunition Plant Marshall, TX 75671	1
Commander Lone Star Army Ammunition Plant Texarkana, TX 75502	1
Commander LA Army Ammo Plant P. O. Box 30,058 Shreveport, LA 71130	1
Commander Milan Army Ammunition Plant Milan, TN 38358	1
Commander Radford Army Ammunition Plant Radford, VA 24141	1

Commander Sunflower Army Ammunition Plant Lawrence, KS 66044	1
Commander Lake City Army Ammunition Plant Attn: Mr. John Jacobi Independence, MO 64056	1
Commander Ravenna Army Ammunition Plant Ravenna, OH 44266	1
Commander Pine Bluff Arsenal Pine Bluff, AR 71601	1
Director US Army Materiel Systems Analysis Activity Aberdeen Proving Ground, MD 21005	3
Director US Army Ballistics Research Laboratories Attn: Mr. R. Vitali Aberdeen Proving Ground, MD 21005	5
Division Engineer US Army Engineer Division, Huntsville Attn: HNDED-R/Mr. Dembo Mr. W. Char P.O. Box 1600, West Station Huntsville, AL 35807	1 ea
US Army Engineer Division Waterways Experimental Station P.O. Box 631 Vicksburg, MS 39180	1
Director USAMC Intern Training Center Attn: Dr. G. Chiang Red River Depot Texarkana, TX 75502	1
Dr. Robert D. Siewert NASA Lewis Laboratory 21000 Brook Park Rd Cleveland, OH 44135	1

Mr. George Pinkas Code 21-4 NASA Lewis Laboratory 21000 Brook Park Rd Cleveland, OH 44135	1
Mr. W. H. Jackson Deputy Manager for Engineering Atomic Energy Commission P.O. Box E Oak Ridge, TN 37830	1
Mr. Erskine Harton US Department of Transportation Washington, DC 20315	1
Dr. Jean Foster US Department of Transportation Washington, DC 20315	1
Mr. Frank Neff Mound Laboratory Monsanto Research Corp. Miamisburg, OH 45342	1
Ms. Trudy Prugh Mound Laboratory Monsanto Research Corp. Miamisburg, OH 45342	1
Commander Naval Weapons Laboratory Attn: Mr. F. Sanches Dahlgren, VA 22448	1
Dr. W. E. Baker Southwest Research Institute San Antonio, TX 78284	1
Division Engineer US Army Engineer Division, Fort Belvoir Fort Belvoir, VA 22060	1
Commander Naval Sea Systems Command Washington, DC 20315	1

Mr. Billings Brown Hercules, Inc. Box 98 Magna, UT 84044	1
Mr. John Komos Defense Supply Agency Cameron Station Alexandria, VA 22030	1
Office of the Project Manager for Chemical Demilitarization and Installation Restoration Edgewood Arsenal Aberdeen Proving Ground, MD 21010	2
Edgewood Arsenal Technical Director Attn: SAREA-TD-E Foreign Intelligence Officer Chief, Legal Office Chief, Safety Office CDR, US Army Technical Escort Center Author's Copy, Manufacturing Technology Directorate Aberdeen Proving Ground, MD 21010	1 1 1 1 1 3
Edgewood Arsenal Director of Biomedical Laboratory Attn: SAREA-BL-M SAREA-BL-B SAREA-BL-E SAREA-BL-H SAREA-BL-R SAREA-BL-T Aberdeen Proving Ground, MD 21010	1 1 1 1 1 1
Edgewood Arsenal Director of Chemical Laboratory Attn: SAREA-CL-C SAREA-CL-P Aberdeen Proving Ground, MD 21010	1
Edgewood Arsenal Director of Development & Engineering Attn: SAREA-DE-S Aberdeen Proving Ground, MD 21010	4

Edgewood Arsenal	
Director of Manufacturing Technology	
Attn: SAREA-MT-TS	2
SAREA-MT-M	1
Aberdeen Proving Ground, MD 21010	
Edgewood Arsenal	
Director of Product Assurance	
Attn: SAREA-PA-A	1
SAREA-PA-P	1
SAREA-PA-Q	1
Aberdeen Proving Ground, MD 21010	
Edgewood Arsenal	
Director of Technical Support	
Attn: SAREA-TS-R	2
SAREA-TS-L	3
SAREA-TS-E	1
Aberdeen Proving Ground, MD 21010	
Aberdeen Proving Ground	
Record Copy	1
CDR, APG	
Attn: STEAP-AD-R/RHA	
APG-Edgewood Area, BLDG E5179	
Aberdeen Proving Ground, MD 21005	
Aberdeen Proving Ground	
CDR, APG	1
Attn: STEAP-TL	
APG, Aberdeen Area	
Aberdeen Proving Ground, MD 21005	
DEPARTMENT OF DEFENSE	
Administrator	
Defense Documentation Center	12
Attn: Accessions Division	
Cameron Station	
Alexandria, VA 22314	
Commander	
Edgewood Arsenal	
Attn: SAREA-DM	1
Aberdeen Proving Ground, MD 21010	